Journal of the American Mosquito Control Association, 15(2):157–185, 1999

A DESCRIPTION AND MORPHOMETRIC COMPARISON OF EGGS OF SPECIES OF THE *ANOPHELES GAMBIAE* COMPLEX

L. P. LOUNIBOS,[1] M. COETZEE,[2] D. DUZAK,[1] N. NISHIMURA,[1] J. R. LINLEY,[1,3] M. W. SERVICE,[4] A. J. CORNEL,[5,6] D. FONTENILLE[7,8] AND L. G. MUKWAYA[9]

ABSTRACT. Eggs of the 6 named species of the *Anopheles gambiae* complex are described from scanning electron micrographs of specimens obtained from laboratory colonies or wild-caught females. Morphometric measurements of eggs from 5 sources of *Anopheles arabiensis,* 2 of *Anopheles gambiae,* one of *Anopheles quadriannulatus,* 2 of *Anopheles bwambae,* 2 of *Anopheles merus,* and one of *Anopheles melas* are compared, and relationships are analyzed by multivariate statistics. No morphologic characters were species-diagnostic, although tendencies of the saltwater species *An. merus* and *An. melas* to have wider decks and shorter floats were confirmed. Species and populations overlapped considerably in principal components and discriminant function analyses based on 10 attributes of eggs. Nevertheless, discriminant functions revealed similarities in eggs of species believed to be most closely related, namely, *An. gambiae* and *An. arabiensis, An. merus* and *An. melas,* and *An. quadriannulatus* and *An. bwambae.*

KEY WORDS Africa, egg attributes, malaria, morphology, scanning electron microscopy, vectors

INTRODUCTION

The *Anopheles gambiae* Giles complex at present contains 6 named species (Gillies and Coetzee 1987), one unnamed species (Hunt et al. 1998), and 3 or 4 incipient species in West Africa (Coluzzi et al. 1985, Favia et al. 1997). Some of the species are extremely efficient vectors of malaria parasites, whereas others are not involved in transmission at all, or are involved in only a limited way at some localities. Morphologic characteristics for identifying the various species are largely lacking (Coetzee 1989), and alternative techniques, such as analyses of polytene chromosome banding arrangements (Coluzzi and Sabatini 1967) and the resolution of species-specific DNA sequences (Scott et al. 1993) are necessary for identification, population studies, and monitoring of malaria control programs. However, useful morphologic characters occur in the egg stage and can be used to separate the saltwater-breeding species *Anopheles merus* Dönitz and *Anopheles melas* Theobald from the other members of the complex (Muirhead Thomson 1945, 1948).

Studies of the egg morphology of other groups of *Anopheles* using scanning electron microscopy (SEM) have proven useful for separating closely related species or geographical trends within species (Linley et al. 1993a, 1993b, 1995, 1996). A discriminant function analysis of egg characteristics of the 5 known species of the *Anopheles quadrimaculatus* Say complex permitted correct classification of 97.7% of the eggs to species (Linley et al. 1993a).

Despite the importance of the *An. gambiae* complex in disease transmission (White 1974, Gillies and Coetzee 1987), eggs of these species have not been examined by SEM, except for a preliminary account by Hinton (1968). The present paper reports results of an SEM study on eggs of the 6 named species of the *An. gambiae* complex.

MATERIALS AND METHODS

Adult females were obtained from laboratory colonies or field collections (Table 1). Bloodfed females were isolated individually for oviposition or, in the case of 5 colonies, eggs were collected from an unknown number of females that oviposited in cages into the same container. The specific identities of the mother or progeny from the same egg batches were determined chromosomally (Hunt 1973) or by polymerase chain reaction–amplification of species-specific regions of DNA (Scott et al. 1993). Where females were individually isolated, 3–5 eggs per female were chosen for SEM.

Approximately 1 day after oviposition, eggs were preserved in alcoholic Bouin's solution for shipment to the Florida Medical Entomology Laboratory. In preparation for SEM, eggs were dried, mounted on stubs, sputter-coated with gold, and examined in a Hitachi S-510 SEM, as described previously (Linley et al. 1993a, 1993b, 1995, 1996).

For each source of specimens (Table 1), selected attributes of 3–18 eggs were measured from micro-

[1] Florida Medical Entomology Laboratory, University of Florida, 200 9th Street SE, Vero Beach, FL 32962.
[2] Department of Medical Entomology, South African Institute for Medical Research, PO Box 1038, Johannesburg 2000, South Africa.
[3] Deceased.
[4] Liverpool School of Tropical Medicine, Pembroke Place, Liverpool L3 5QA, United Kingdom.
[5] Entomology Branch, Division of Parasitic Diseases, Mailstop F22, Centers for Disease Control and Prevention, 4770 Buford Highway, Chamblee GA 30341.
[6] Present address: Department of Entomology, University of California, Mosquito Control Research Laboratory, 9240 S Riverbend Avenue, Parlier, CA 93648.
[7] Laboratoire de Zoologie Medicale, ORSTOM–Institut Pasteur, BP 220, Dakar, Senegal.
[8] Present address: OCEAC, BP 288, Yaoundé, Cameroun.
[9] Mosquito Research Programme, Uganda Virus Research Institute, PO Box 49, Entebbe, Uganda.

Table 1. Geographic origin and colony or collection history of *Anopheles gambiae* complex mosquitoes used for the present study.

Species	Geographic origin	Coordinates	Code[1]	Date colonized or collected	No. females[2]	No. eggs
An. gambiae	McCarthy Island, The Gambia	13°31′N, 14°49′W	G3	1975	6	18
An. gambiae	Bagamoyo, Tanzania	6°26′S, 38°55′E	KOG	1992	Colony	15
An. arabiensis	Dakar, Senegal	14°38′N, 17°27′W	DAKAR	1993	6	18
An. arabiensis	Maputo, Mozambique	25°52′S, 32°30′E	MA	1990	Colony	15
An. arabiensis	Senna, Sudan	13°30′N, 33°50′E	SUD	1992	1	3
An. arabiensis	Kanyemba, Zimbabwe	15°40′S, 30°20′E	KGB	1975	1	3
An. arabiensis	Ahero, Kenya	0°18′S, 34°45′E	KEN	1991	4	12
An. quadriannulatus	Skukuza, S. Africa	24°59′S, 31°35′E	SKUQUA	1995	Colony	15
An. bwambae	Mongiro, Uganda	0°50′N, 30°50′E	MON	1993	4	17
An. bwambae	Kyakatimba, Uganda	0°50′N, 30°50′E	KYA	1995	3	9
An. merus	Dar Es Salaam, Tanzania	6°51′S, 39°18′E	MERDAR	1992	Colony	15
An. merus	Mafayeni, South Africa	23°01′S, 31°15′E	MAF	1989	Colony	15
An. melas	Djifer, Senegal	14°04′N, 16°52′W	DJI	1996	3	10

[1] G3, KOG, DAKAR, MA, KGB, SKUQUA, MERDAR, and MAF are previously published acronyms used to denote these colonies.
[2] Eggs for scanning electron microscopy were obtained from individual ovipositions except for sources designated as colony.

graphs with a digitizing tablet and SigmaScan software (Jandel Scientific, San Rafael, CA). Attributes measured were as in Linley et al. (1995, 1996), with the omission of certain variables, such as those associated with chorionic cell areas, which were not recorded because of the indistinct cell boundaries in some species of the *An. gambiae* complex. Explanations of acronyms used to identify attributes are provided in the Appendix. Two float attributes of eggs of *Anopheles bwambae* White from KYA were not measured because of damage to these specimens.

Statistical analyses of attributes were performed without adjustments for a priori specific identifications. Thus, specimen source (colony or collection site) was used as the dependent variable in a series of one-way analyses of variance, performed with PROC GLM of SAS (SAS Institute Inc. 1985), followed by the REGWQ multiple comparisons procedure to test for significant differences among site means for each attribute.

Multivariate analyses used only 10 of the 23 measured attributes, relying on variables such as ratios and direct counts, known to be less affected by female or egg size (Linley et al. 1993a). Principle component analysis was performed using default settings of PROC PRINCOMP of SAS (SAS Institute Inc. 1985), and discriminant function analysis was performed with Statgraphics software (Statgraphics 1992). Both procedures have been used previously on egg attributes to separate closely related species or geographic populations (Linley et al. 1993a, 1993b, 1995, 1996).

Species-specific descriptions were based on micrographs from a unique collection or colony, determined for species from multiple sites (Table 1) by specimen quality and abundance. Following the complete description of *An. gambiae* Giles, subsequent descriptions are abridged where characters did not differ from those of *An. gambiae* s.s.

RESULTS

Egg of *Anopheles gambiae* Giles (G3)

Size: As in Table 2.

Color: Black.

Overall appearance: Boat-shaped in ventral and lateral views, anterior and posterior ends blunt (Figs. 1 and 2a, 2d). Ventral surface concave, especially near midline (Fig. 1b); dorsal surface curved, more acutely near ends. Float centered near midline in lateral view (Fig. 1b), extending approximately ⅔ total length of egg (Table 2).

Ventral (upper) surface: Deck continuous along length of egg, relatively equal in width throughout, constricting at anterior and posterior poles (Figs. 1a and 2a, 2d). Frill moderate in height across length of egg (Fig. 1b). Chorionic cell outlines not visible on deck, tubercle distribution similar in anterior, middle, and posterior regions (Figs. 3a–3c). Individual tubercles elevated, dome-shaped, with buttressed ridges on sides (Fig. 3d). Ventral plastron cells limited to ridge between float and frill (Figs. 1a and 3e), pores fewer and reticulum less distinct than in dorsal plastron (Figs. 3e, 3i).

Lobed tubercles more numerous at anterior end of egg (Table 2), where frill is less indented than at posterior pole (Figs. 2b, 2e). Shape of lobed tubercles oval or elliptical (Figs. 2b, 2f), lobes sometimes swollen at ends, variable in number.

Dorsal (lower) and lateral surfaces: Chorionic cell structure not visible on dorsal surface (Fig. 3g).

Plastron pores irregular in size, fewer and smaller near dorsal float margins (Figs. 3f–3h), connected by filamentous or broad bridges (Fig. 3i). Chorionic cell boundaries more apparent in lateral or end-on views, polygonal in shape (Figs. 1b and Figs. 2b, 2e). Ribs in center of float bifurcate to form lobes (Fig. 1b).

Anterior end, micropyle: Anterior end rounded, frill undulating at borders with lobed tubercles (Figs. 2a, 2b). Micropylar collar smooth, occasionally punctuated with holes, usually separated from frill margin by plastron (Figs. 2b, 2c). Micropylar collar irregularly rounded with internal hexagonal rays extending radially inward to orifice (Fig. 2c). Disk surface slightly rugose, orifice at center of low mound.

Posterior end: Rounded, with a flap of plastron cells overlapping ventral surface such that lobed tubercles are displaced further from end than at anterior pole (Figs 2d, 2e).

Quantitative comparison with KOG An. gambiae: A posteriori means comparisons revealed that eggs from the Gambian (G3) colony were significantly longer and wider than counterparts from the Tanzanian (KOG) colony (Table 2). So, too, were means for float length, float length per rib, whole egg area, and anterior tubercle density significantly greater for the Gambian *An. gambiae*. In contrast, mean number of lobed tubercles, both anterior and total, and total micropyle area were significantly greater in the specimens from the Tanzanian colony.

Egg of *Anopheles arabiensis* Patton (DAKAR)

Size: As in Table 2.

Color: Black.

Overall appearance: Ventral and lateral views and anterior and posterior ends as in *An. gambiae* (Figs. 4 and 5a, 5d). Ventral surface and floats as in *An. gambiae* (Fig. 4b).

Ventral (upper) surface: Deck continuous along length of egg, slightly constricted near midline in some specimens (Fig. 4a), narrowing at poles (Figs. 5a, 5b, 5d, 5e). Frill (Fig. 4b), chorionic cell outlines, and tubercle distribution (Figs. 6a–6c) as in *An. gambiae*. Some anterior deck tubercles highly elongated and undulant, anchored from buttressed roots (Fig. 6d). Ventral plastron in narrow ridge between frill and float, lateral to which tubercles are exposed where float separates from egg (Fig. 6e).

Lobed tubercles and frill at anterior end as in *An. gambiae* (Figs. 5a, 5b). Deck tubercles more elongate in vicinity of lobed tubercles (Fig. 5f).

Dorsal (lower) and lateral surfaces: Chorionic cell structure sometimes visible on dorsal surfaces, boundaries defined by raised mounds (Fig. 6g). Plastron pores (Figs. 6f, 6h, 6i) and chorionic cell boundaries (Figs. 4b and 5b, 5e) as in *An. gambiae*.

Anterior end, micropyle: Anterior end and frill as in *An. gambiae*, but inner margin of micropylar collar more evenly rounded (Figs. 5a, 5b, 5c). Surface of micropylar disk faintly striated, orifice at center of low mound (Fig. 5c).

Posterior end: As in *An. gambiae* (Figs. 5d, 5e).

Quantitative comparisons of attributes from 5 sources of An. arabiensis *eggs*: Significant differences were detected in mean egg lengths and widths, but not among ratios of these variables (Table 2). Among float attributes, specimens from the Sudan and Zimbabwe had significantly fewer mean numbers of ribs than other *An. arabiensis*, and significant differences in float length per rib were detected. Significant intraspecific differences were recorded for all 4 deck dimensions, but in none of the 4 properties of lobed tubercles. Anterior deck tubercle density was significantly less for Zimbabwean (KGB) *An. arabiensis*, and significant differences among means of 3 micropyle properties were found among the 5 sources of this species.

Egg of *Anopheles quadriannulatus* (Theobald) (SKUQUA)

Size: As in Table 2.

Color: Black.

Overall appearance: As in *An. gambiae* (Figs. 7 and 8a, 8d), including relationship of float to total length of egg (Table 2).

Ventral (upper) surface: Deck as in *An. gambiae* (Figs. 7a and 8a, 8d). Frill moderate to high across length of egg (Fig. 7b). Chorionic cell outlines and tubercle distributions as in *An. gambiae* (Figs. 9a–9c). Tubercles varying in shape from domed, some with pits, to asteroid; buttressed ridges common (Figs. 9a–9d). Ventral plastron between floats and frill as in *An. gambiae*, with large pores at border with frill (Fig. 9e).

Lobed tubercles at both ends of egg, where frill reduced in height (Figs. 8b, 8e). Shape of lobed tubercles oval to elliptical (Fig. 8f), lobes constant in width or swollen at ends. Deck tubercles less dense and more elongate among lobed tubercles (Fig. 8f).

Dorsal (lower) and lateral surfaces: Chorionic cell boundaries, described by round protuberances, polygonal and most visible at ends of egg (Figs. 7b and 8b, 8e). Plastron pores as in *An. gambiae* (Figs. 9e, 9f), connected by broad or narrow bridges (Figs. 9g–9i).

Anterior end, micropyle: Anterior end rounded, frill reduced where abutting on lobed tubercles (Fig. 8b). Micropylar collar and disk as in *An. gambiae* (Figs. 8b, 8c). Disk surface relatively smooth, orifice at center of low mound.

Posterior end: Rounded, with a dense layer of plastron cells bordering and posterior to lobed tubercles (Figs. 8d, 8e).

Table 2. Means[1] and standard errors for 23 attributes[2] of eggs of *Anopheles gambiae* complex mosquitoes measured from 13 sources.

Attribute	*An. gambiae*		*An. arabiensis*	
	G3	KOG	KEN	MA
	(n = 18)	(n = 15)	(n = 12)	(n = 15)
Linear dimensions[3]				
Egglen	504.6 ± 6.2 abc	443.8 ± 4.6 d	495.4 ± 2.3 abc	500.1 ± 10.1 abc
Eggwid	172 ± 3.3 ab	153.6 ± 2.4 c	163.8 ± 2.9 bc	175.5 ± 2.9 ab
Lenwidrat	2.9 ± 0.1 bcd	2.9 ± 0.05 cd	3 ± 0.05 abcd	2.9 ± 0.1 cd
Float attributes				
Mnfltlen	343.9 ± 5.9 a	284.7 ± 5.4 c	318.1 ± 3.1 abc	322 ± 8.6 abc
Fltpcn	68.1 ± 0.6 ab	64.1 ± 0.9 abc	64.2 ± 0.6 abc	64.3 ± 0.8 abc
Mnribs	22.7 ± 0.4 bcd	23.7 ± 0.4 abcd	23 ± 0.4 abcd	25.6 ± 0.9 ab
Fltlenprib	15.2 ± 0.4 a	12 ± 0.1 e	13.9 ± 0.3 abcd	12.7 ± 0.2 cde
Deck dimensions[4]				
Arwhlegg	65,999.05 ± 1,453.84 abcd	53,369.9 ± 1,122.16 e	60,989.48 ± 976.27 cde	67,204.4 ± 1,812.07 abc
Artotdk	30,188.08 ± 983.48 abc	27,797.58 ± 433.9 cd	24,833.77 ± 1,542.73 d	29,024.27 ± 1,017.91 bcd
Totdkpcn	45.92 ± 1.43 cde	52.58 ± 0.97 abc	40.74 ± 2.44 ef	43.56 ± 1.85 def
Dkwidpcn	40.4 ± 1.77 abc	40.57 ± 0.98 abc	32.08 ± 2.76 cde	34.63 ± 1.72 bcde
Lobed tubercles				
		(n = 30)		(n = 30)
Noantlobtb	5.5 ± 0.35 bc	8.73 ± 0.27 a	5 ± 0.25 c	6.23 ± 0.19 bc
Noposlobtb	4.89 ± 0.16 abc	6 ± 0.14 a	4.58 ± 0.26 c	5.1 ± 0.13 abc
Totnolobtb	10.39 ± 0.43 cd	14.73 ± 0.28 a	9.58 ± 0.34 d	11.33 ± 0.24 bcd
Antposlobrat	1.13 ± 0.07 ab	1.49 ± 0.07 a	1.14 ± 0.09 ab	1.24 ± 0.05 ab
Anterior deck tubercles				
Anttbden[5]	89.8 ± 3.1 a	69.8 ± 3.2 bcd	75.1 ± 2.8 b	67.6 ± 3.7 bcde
Mnanttbar	1.62 ± 0.06 dc	1.99 ± 0.09 d	1.27 ± 0.06 d	1.65 ± 0.1 dc
Mnanttbfm[6]	0.357 ± 0.019 c	0.217 ± 0.029 cd	0.258 ± 0.007 cd	0.222 ± 0.009 cd
Micropyle				
	(n = 12)	(n = 30)	(n = 8)	(n = 17)
Totarmic	507.5 ± 20.2 d	663.5 ± 14.6 ab	593.2 ± 23.5 bcd	617.7 ± 16.3 bcd
Colarmic	319.7 ± 16.6 cd	406.7 ± 8.3 abc	356.3 ± 10.1 bcd	402.8 ± 10.3 abc
Dskarmic	187.8 ± 9.8 b	256.9 ± 8.3 ab	236.8 ± 16 ab	214.9 ± 9.6 ab
Dskarpcn	37.2 ± 1.7 abc	38.5 ± 0.7 abc	39.7 ± 1.4 ab	34.6 ± 1 bc
	(n = 30)	(n = 30)	(n = 8)	(n = 30)
Nosect	6.2 ± 0.2 a	6.6 ± 0.1 a	6.8 ± 0.2 a	6.3 ± 0.1 a

[1] Means within rows followed by the same letter do not differ significantly ($P > 0.05$ by REGWQ of SAS Institute, Inc. [1985]).
[2] Attributes are defined in the Appendix.
[3] All linear measurements in μm.
[4] All area measurements in μm².
[5] Number in an area of 400 μm².
[6] Form factor = 4π(area/perimeter²).

Table 2. Extended.

An. arabiensis (continued)			*An. quadriannulatus*
SUD	ZIM	DAKAR	SKUQUA
(n = 3)	(n = 3)	(n = 15)	(n = 14)
471.1 ± 6.5 cd	522.2 ± 6.7 a	482 ± 3.9 bc	477.7 ± 6.5 bcd
162.8 ± 2.9 bc	182.1 ± 6.4 a	161.5 ± 2.5 bc	171.9 ± 2.6 ab
2.9 ± 0.1 cd	2.9 ± 0.1 cd	3 ± 0.04 bcd	2.8 ± 0.04 d
314.1 ± 7.1 abc	327.9 ± 6.9 ab	310.9 ± 5.1 abc	315.5 ± 6.9 abc
66.7 ± 1.6 ab	62.8 ± 1.6 bcd	64.5 ± 0.9 abc	66 ± 1.1 ab
21.8 ± 0.4 cd	21.5 ± 0.8 cd	25 ± 0.5 abc	24.1 ± 0.7 abcd
14.4 ± 0.6 abc	15.3 ± 0.7 a	12.5 ± 0.2 de	13.2 ± 0.3 bcde
57,945.8 ± 136.87 de	71,260.2 ± 1,239 a	61,248.5 ± 1,209.4 cde	61,502.97 ± 1,455.65 cde
29,662.3 ± 1,370.7 abcd	34,192.7 ± 2,572.6 a	28,052.5 ± 483.52 cd	26,506.9 ± 616.6 cd
51.18 ± 2.24 abcd	47.89 ± 2.74 bcde	46.03 ± 1.13 cde	43.24 ± 0.98 ef
43.64 ± 2.78 ab	35.97 ± 1.28 bcd	35.73 ± 1.18 bcd	34.61 ± 1.33 bcde
		(n = 30)	
5.67 ± 0.33 bc	6.33 ± 0.33 bc	6.2 ± 0.18 bc	5.79 ± 0.24 bc
4.67 ± 0.33 bc	4.67 ± 0.67 bc	5.17 ± 0.14 abc	5.5 ± 0.25 abc
10.33 ± 0.33 cd	11 ± 1 bcd	11.37 ± 0.25 bcd	11.29 ± 0.45 bcd
1.23 ± 0.15 ab	1.39 ± 0.11 ab	1.22 ± 0.04 ab	1.06 ± 0.04 b
59 ± 4 bcdef	50 ± 7.4 f	74.4 ± 2.3 bc	51.4 ± 2.4 ef
1.61 ± 0.21 dc	1.99 ± 0.09 bcd	1.24 ± 0.05 d	2.59 ± 0.21 ab
0.203 ± 0.011 d	0.217 ± 0.029 cd	0.187 ± 0.0007 d	0.257 ± 0.019 cd
(n = 2)	(n = 2)	(n = 16)	(n = 8)
646.3 ± 21.5 abc	750.7 ± 48.8 a	631.4 ± 28.3 abcd	591.4 ± 17.7 bcd
404 ± 11.7 abc	485.8 ± 51.5 a	423.3 ± 17.5 ab	361.2 ± 12 bcd
242.3 ± 9.8 ab	264.9 ± 2.7 a	208.1 ± 12 ab	230.3 ± 11.3 ab
37.5 ± 0.3 abc	35.5 ± 2.7 bc	32.7 ± 0.7 c	38.9 ± 1.3 abc
(n = 2)	(n = 2)	(n = 30)	(n = 20)
6.5 ± 0.5 a	6 ± 0 a	6.5 ± 0.1 a	6.5 ± 0.2 a

Table 2. Extended.

An. bwambae		*An. merus*		*An. melas*
MON	KYA	MAF	MERDAR	DJI
(n = 17)	(n = 9)	(n = 15)	(n = 15)	(n = 10)
512.1 ± 7.2 ab	506.2 ± 5.6 abc	514.8 ± 5.4 ab	498.8 ± 7.1 abc	493.4 ± 11.7 abc
176.6 ± 2.3 ab	152.4 ± 4.9 c	162.2 ± 3.3 bc	159.4 ± 2.8 bc	152.7 ± 4.1 c
2.9 ± 0.04 cd	3.3 ± 0.1 a	3.2 ± 0.07 abc	3.1 ± 0.05 abc	3.2 ± 0.04 ab
347.8 ± 5.9 a	349.8 ± 5.4 a	303.2 ± 6.6 bc	283.5 ± 6.7 c	296.3 ± 16.1 bc
67.9 ± 0.5 ab	69.1 ± 0.6 a	58.8 ± 1 de	56.9 ± 1.1 e	59.7 ± 2 cde
26.2 ± 0.5 a	Not measured	21 ± 0.7 d	21.6 ± 0.6 cd	21.9 ± 0.7 cd
13.3 ± 0.2 bcde	Not measured	14.6 ± 0.4 ab	13.2 ± 0.3 bcde	13.5 ± 0.6 abcde
70,315.23 ± 1,489.7 ab	61,885.43 ± 1,714.91 bcde	62,952.7 ± 1,349.3 abcd	60,004.2 ± 1,685.3 cde	58,641.61 ± 2,868.48 cde
25,520.43 ± 945.28 cd	24,760.44 ± 530.76 d	34,785.8 ± 728.53 a	33,170.5 ± 1,069.4 ab	33,543.09 ± 948.75 ab
36.32 ± 1.09 f	40.19 ± 1.14 ef	55.42 ± 1.11 ab	55.39 ± 1.24 ab	57.79 ± 1.49 a
26.31 ± 1.63 e	29.82 ± 1.49 de	43.64 ± 1.47 ab	43.64 ± 1.14 ab	47.68 ± 1.07 a
		(n = 30)	(n = 30)	(n = 17)
5.47 ± 0.19 bc	5 ± 0.24 c	6.4 ± 0.15 bc	6.97 ± 0.19 b	5.94 ± 0.3 bc
5.29 ± 0.24 abc	4.78 ± 0.28 bc	5.77 ± 0.11 ab	5.53 ± 0.16 abc	5.53 ± 0.21 abc
10.76 ± 0.34 bcd	9.78 ± 0.49 d	12.17 ± 0.17 bc	12.5 ± 0.31 b	11.47 ± 0.41 bcd
1.06 ± 0.05 b	1.06 ± 0.04 b	1.13 ± 0.04 ab	1.27 ± 0.03 ab	1.09 ± 0.06 b
55.1 ± 2.7 def	53.6 ± 2.6 def	61.9 ± 2.1 bcdef	64.7 ± 1.6 bcdef	58.4 ± 1.3 cdef
2.91 ± 0.23 a	2.29 ± 0.16 abc	1.35 ± 0.05 d	1.24 ± 0.07 d	1.75 ± 0.09 dc
0.483 ± 0.057 b	0.652 ± 0.022 a	0.216 ± 0.007 cd	0.238 ± 0.013 cd	0.229 ± 0.015 cd
(n = 8)	(n = 6)	(n = 30)	(n = 30)	(n = 17)
587.8 ± 11.5 bcd	571 ± 19.6 bcd	660.6 ± 17.8 ab	568.7 ± 10.3 bcd	520.8 ± 15.1 cd
335.9 ± 13.6 bcd	342 ± 12.7 bcd	410.2 ± 12.5 ab	367.8 ± 7.2 bcd	294 ± 7.9 d
252 ± 11.8 ab	229 ± 18.7 ab	250.3 ± 6.7 ab	201 ± 5.8 ab	226.8 ± 8.6 ab
42.9 ± 1.9 a	39.9 ± 2.3 ab	38 ± 0.5 abc	35.3 ± 0.7 bc	43.4 ± 0.8 a
(n = 20)	(n = 11)	(n = 30)	(n = 30)	(n = 11)
6.2 ± 0.1 a	6.5 ± 0.2 a	6.5 ± 0.1 a	6.3 ± 0.1 a	6.5 ± 0.2 a

Egg of *Anopheles bwambae* White (MON)

Size: As in Table 2.

Color: Black.

Overall appearance: Ventral and lateral views and anterior and posterior ends as in *An. gambiae* (Figs. 10 and 11a, 11d). Ventral surface concave (Fig. 10b), dorsal surface more curved near poles, especially anteriorly (Fig. 10b).

Ventral (upper) surface: Deck continuous along length of egg, narrowing at midline and at poles (Fig. 10a). Frill moderate in height (Fig. 10b), terminating at ends (Figs. 11b, 11e). Chorionic cell outlines and tubercle distribution as in *An. gambiae* (Figs. 12a–12c). Buttressed ridges common to most tubercles, some of which have pitted domes (Figs. 12a–12d). Ventral plastron occupies ridge between frill and float, where rounded tubercles define chorionic cell boundaries (Fig. 12e).

Lobed tubercles at both ends of egg as in *An. gambiae* (Figs. 11a, 11d). Deck tubercles more elongate, less domed, in vicinity of lobed tubercles (Fig. 11f).

Dorsal (lower) and lateral surfaces: Chorionic cell structure not visible on dorsum (Figs. 12g, 12h) but visible at ends of egg, where large, rounded tubercles define polygonal boundaries (Figs. 11b, 11e). Plastron pores as in *An. gambiae* (Fig. 12f), connected by anastomosing bridges, some plastron pores in islets (Fig. 12i).

Anterior end, micropyle: Frill anterior to lobed tubercles smothered by plastron (Fig. 11b). Micropylar collar, disk, and orifice as in *An. gambiae* (Fig. 11c).

Posterior end: Smooth, with a dense plastron ridge, with few pores, appressed vertically, forming a border with lobed tubercles (Fig. 11e).

Quantitative comparison with KYA An. bwambae: Mean egg width was significantly less for KYA eggs, hence, the mean length to width ratio from this site was significantly greater (Table 2). No other interspecific comparison between collection sites was significantly different, except for the mean anterior tubercle form factor, because tubercles from KYA eggs were more elongated and less rounded than tubercles from MON eggs.

Egg of *Anopheles merus* Dönitz (MERDAR)

Size: As in Table 2.

Color: Black.

Overall appearance: Ventral and lateral views and anterior and posterior ends as in *An. gambiae* (Figs. 13 and 14a, 14d). Floats slightly shorter than ⅔ total length of egg (Table 2).

Ventral (upper) surface: Deck continuous along length of egg, constricting at poles in all specimens and at midline in some (Fig. 13a). Chorionic cell outlines, tubercle distribution and shape, and ventral plastron as in *An. gambiae* (Figs. 15a–15e, 15h).

Lobed tubercles at both anterior and posterior ends of egg (Figs. 14a, 14d), their shape as in *An. gambiae* (Fig. 14f). Deck tubercles less dense around lobed tubercles, which are bordered on their sides by a lattice (Fig. 14f).

Dorsal (lower) and lateral surfaces: Chorionic cell structure faintly visible in dorsal views (Figs. 15g, 15h) and more apparent in end-on views, which show cell boundaries as polygonal (Figs. 14b, 14e). Plastron pores as in *An. gambiae* (Figs. 15f–15i).

Anterior end, micropyle: Anterior end rounded, frill reduced or overlain with plastron cells at borders with lobed tubercles (Fig. 14f). Micropylar collar, disk, and orifice as in *An. gambiae* (Figs. 14b, 14c).

Posterior end: Rounded, with thick ridge of plastron bordering on lobed tubercles (Figs. 14e, 14f).

Aberrant eggs: Eggs were observed whose deck region was overlain with a variable cover of plastron, with the deck exposed patchily in elliptical or oval areas of different sizes (Fig. 16a). Tubercles exposed in ellipses were surrounded by a ridged frill and within these patches appeared similar to ordinary deck tubercles (Fig. 16b). These aberrant eggs occurred in the same clutch as apparently normal ones.

Quantitative comparison to MAF An. merus: No significant differences were found between *An. merus* from the 2 sites in mean values of any of the 23 measured attributes.

Eggs of *Anopheles melas* Theobald (DJI)

Size: As in Table 2.

Color: Black.

Overall appearance: Ventral and lateral surfaces, anterior and posterior ends, and floats as in *An. gambiae* (Figs. 17 and 18a, 18d). Floats slightly shorter than ⅔ total egg length (Table 2).

Ventral (upper) surface: Deck continuous along length of egg, constricting at poles in all specimens and at midline in some (Fig. 17a). Frill (Fig. 17b), absence of chorionic cell outlines (Figs. 18a, 18d), and tubercle distribution as in *An. gambiae* (Figs. 19a–19c). Largest tubercles dome-shaped, with buttressed ridges on sides, some with pits in domes (Figs. 19b–19d).

Ventral plastron between float and frill as in *An. gambiae* (Fig. 19e). Lobed tubercles at both ends of egg, bordered by frill anteriorly and plastron ridge posteriorly (Figs. 18b, 18e). Shape of lobed tubercles as in *An. gambiae* (Fig. 18f). Deck tubercles less dense between lobed tubercles (Fig. 18f).

Dorsal (lower) and lateral surfaces: Chorionic cells polygonal in shape, best observed in lateral view, borders outlined by protuberant, round tubercles (Fig. 17b). Plastron pores as in *An. gambiae* (Figs. 19f–19i).

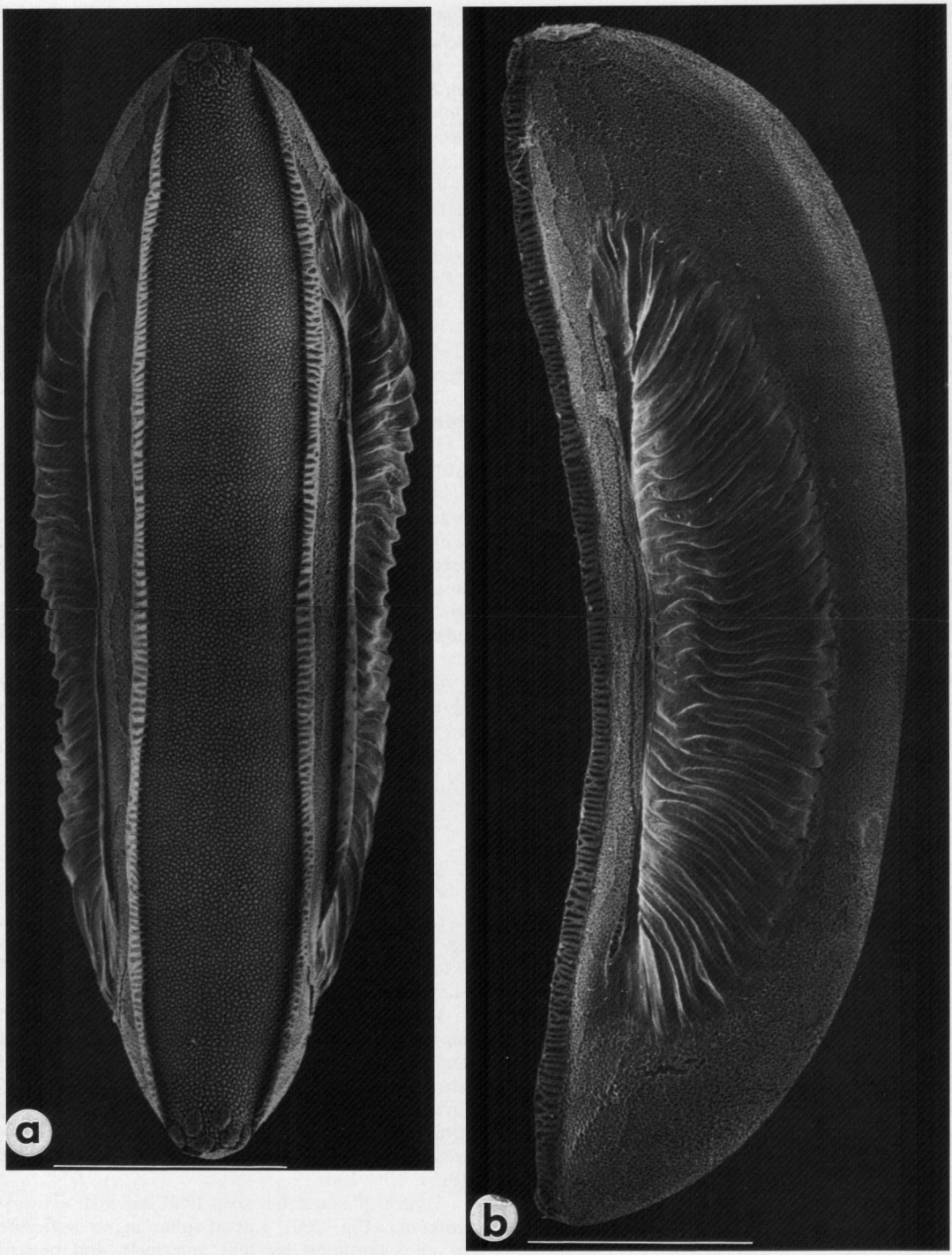

Fig. 1. *Anopheles gambiae* G3 (colony). a. Entire egg, ventral (upper) view, anterior end at top. b. Entire egg, lateral view, ventral surface at left, anterior end at top. Scale = 100 μm.

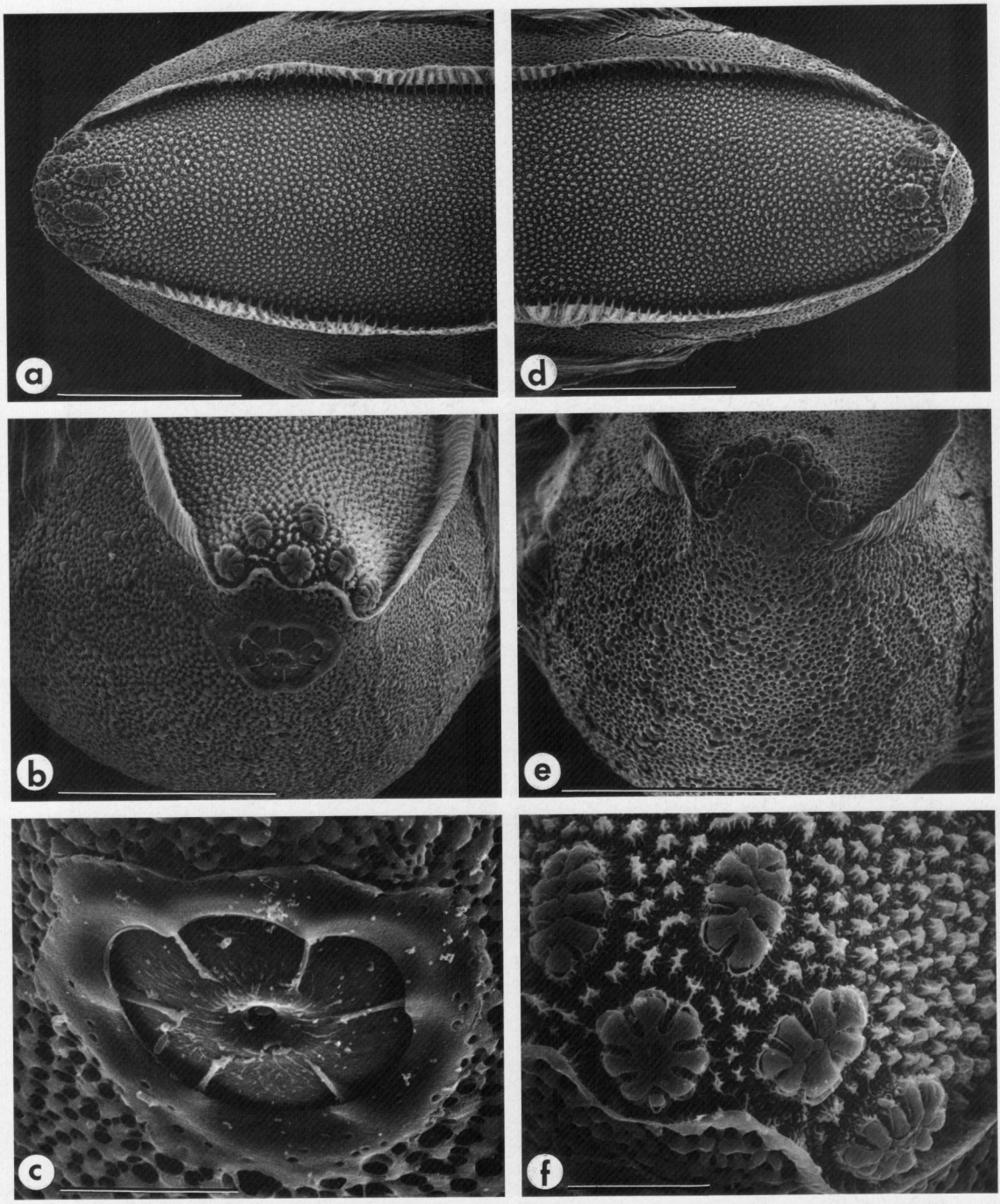

Fig. 2. *Anopheles gambiae* G3 (colony). a. Anterior end, ventral (upper) surface. b. Anterior, end-on view. c. Detail of micropylar apparatus. d. Posterior end, ventral surface. e. Posterior, end-on view. f. Detail, lobed tubercles, anterior end. Scales: a, b, d, e = 50 μm; c, f = 10 μm.

Anterior end, micropyle: Anterior end rounded, frill reduced where it separates lobed tubercles from micropyle (Figs. 18b, 18c). Micropylar collar, disk, and orifice as in *An. gambiae* (Figs. 18b, 18c).

Posterior end: As in *An. gambiae* (Fig. 18e).

Univariate comparisons of attributes among species

Among linear dimensions, intraspecific variation was as extensive as interspecific variation for

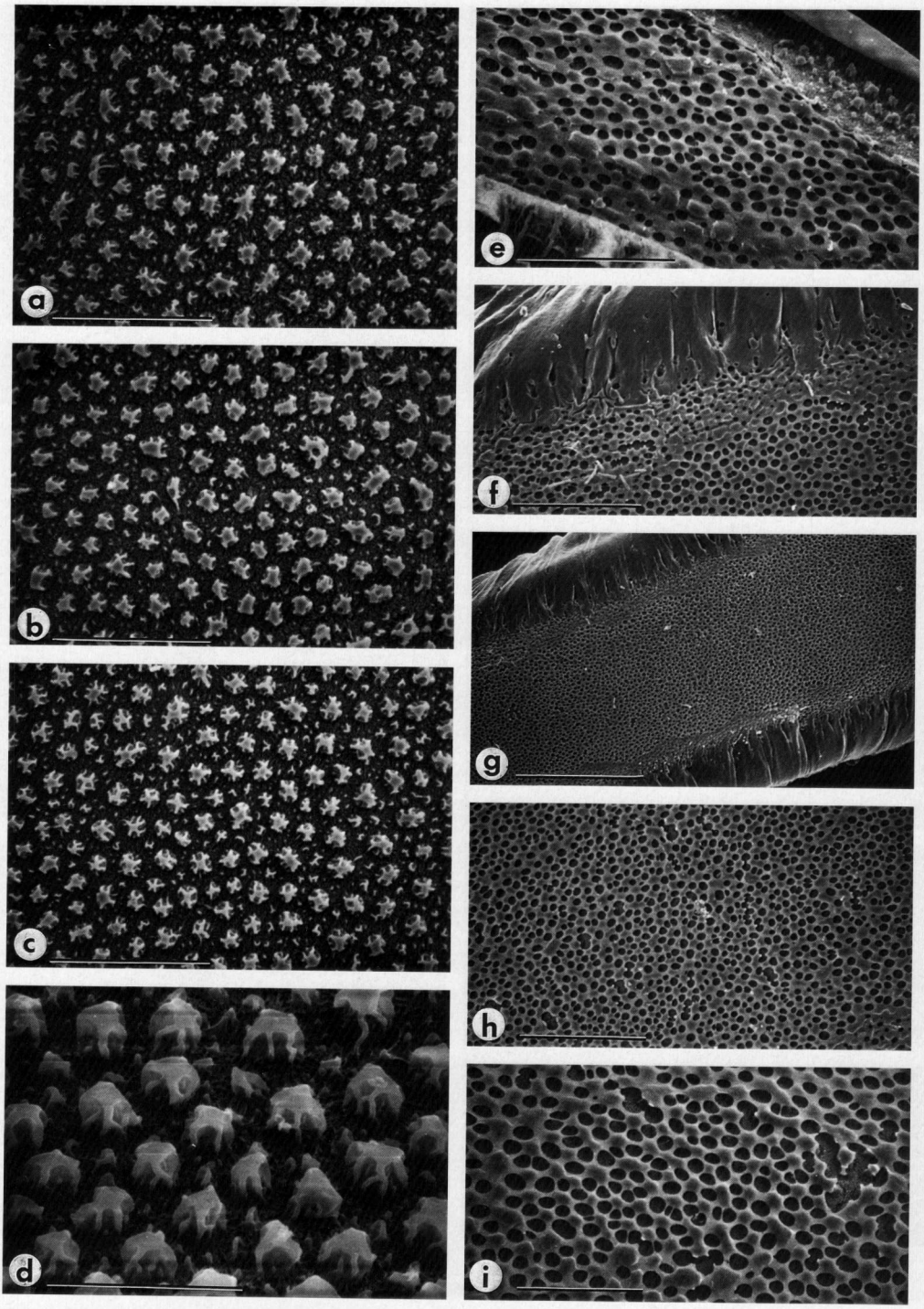

Fig. 3. *Anopheles gambiae* G3 (colony). a. Chorionic tubercles, anterior deck. b. Tubercles, middle deck. c. Tubercles, posterior deck. d. Detail of anterior deck tubercles. e. Plastron between frill (bottom) and float (top). f. Float dorsal margin, transition to plastron. g. Dorsal surface, middle of egg. h, i. Detail, dorsal surface. Scales: a–c, e, i = 10 μm; d = 5 μm; f, h = 20 μm; g = 50 μm.

Fig. 4. *Anopheles arabiensis* DAKAR (colony). a. Entire egg, ventral (upper) view, anterior end at top. b. Entire egg, lateral view, ventral surface at left, anterior end at top. Scale = 100 μm.

most attributes, especially for *An. arabiensis* and *An. gambiae* (Table 2). For float attributes, no significantly different means were found that characterized species. However, means of float length as a percentage of total egg length and mean number of ribs of the saltwater species were significantly less than those of most other samples. Broad variation was also apparent in interspecies comparisons of deck dimensions, although means of deck area as a percentage of whole egg area and deck width as a percentage of total width tended to be largest in *An. merus* and *An. melas* and smallest in *An. bwambae* and *An. quadriannulatus.* Numbers of lobed tubercles

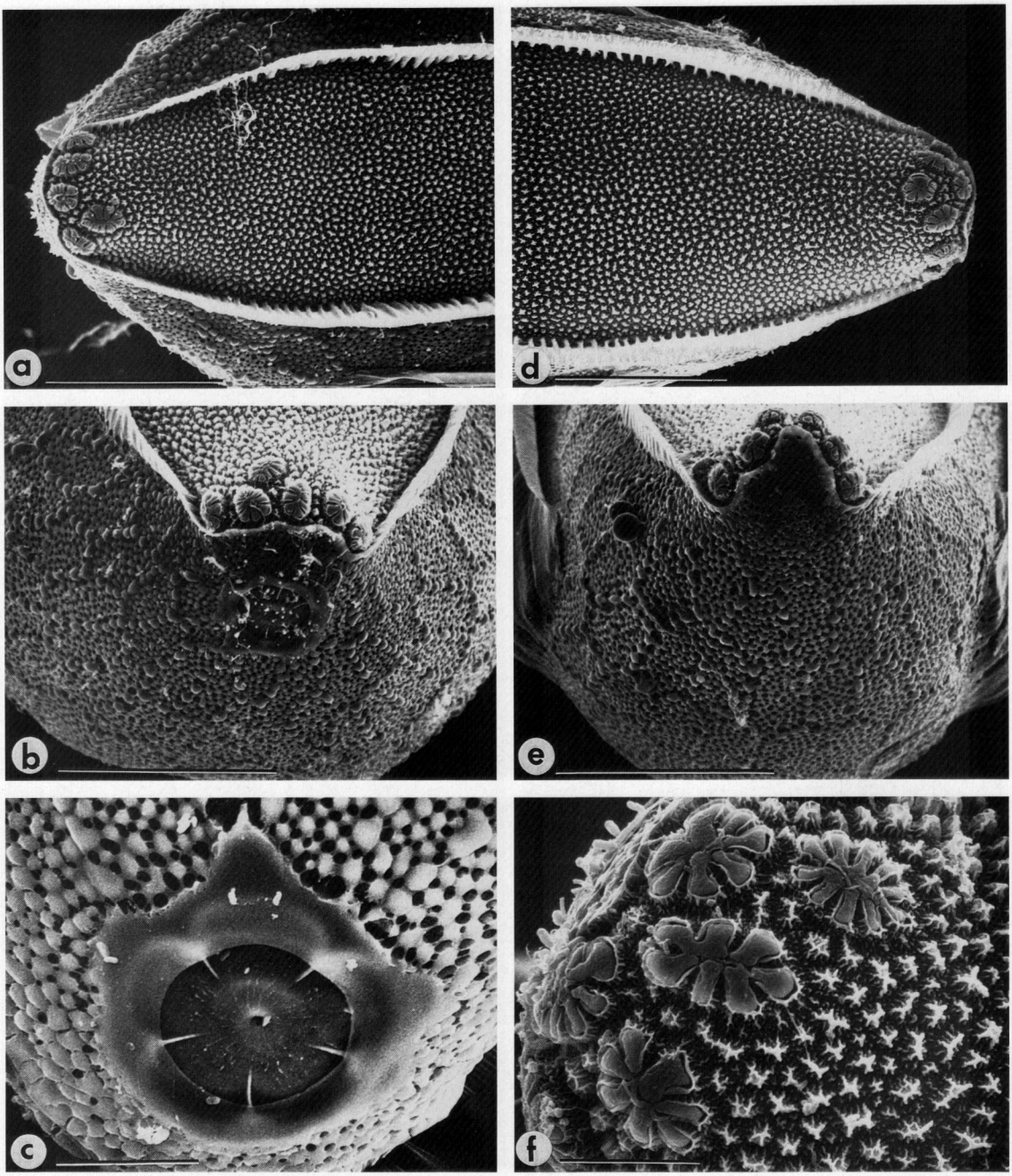

Fig. 5. *Anopheles arabiensis* DAKAR (colony). a. Anterior end, ventral (upper) surface. b. Anterior, end-on view. c. Detail of micropylar apparatus. d. Posterior end, ventral surface. e. Posterior, end-on view. f. Detail, lobed tubercles, anterior end. Scales: a, b, d, e = 50 μm; c, f = 10 μm.

were not valuable discriminatory attributes at the species level. Among attributes of anterior deck tubercles, mean area was significantly greater for *An. bwambae* and *An. quadriannulatus* compared to the other species, and the mean form factor for *An. bwambae* was significantly greater than means of this variable for other samples. Attributes of the micropyle were, in general, not highly differentiated among species or sites, although significant intraspecific differences were detected among mean values for the collar area and total area of the micropyle.

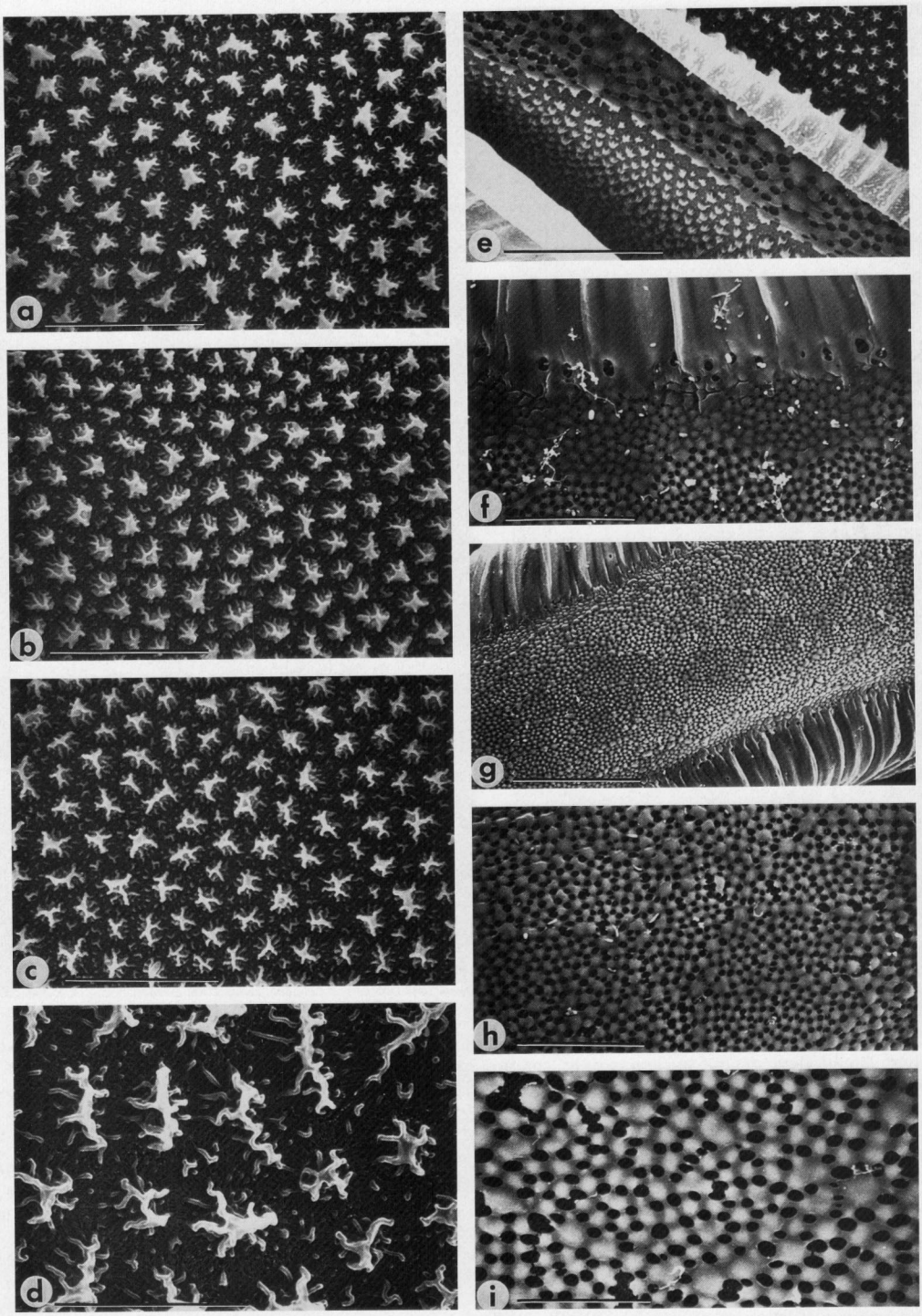

Fig. 6. *Anopheles arabiensis* DAKAR (colony). a. Chorionic tubercles, anterior deck. b. Tubercles, middle deck. c. Tubercles, posterior deck. d. Detail of anterior deck tubercles. e. Plastron between deck and frill (top) and exposed tubercles beneath float (bottom). f. Float dorsal margin, transition to plastron. g. Dorsal surface, middle of egg. h, i. Detail, dorsal surface. Scales: a–c, i = 10 μm; d = 5 μm; e, f, h = 20 μm; g = 50 μm.

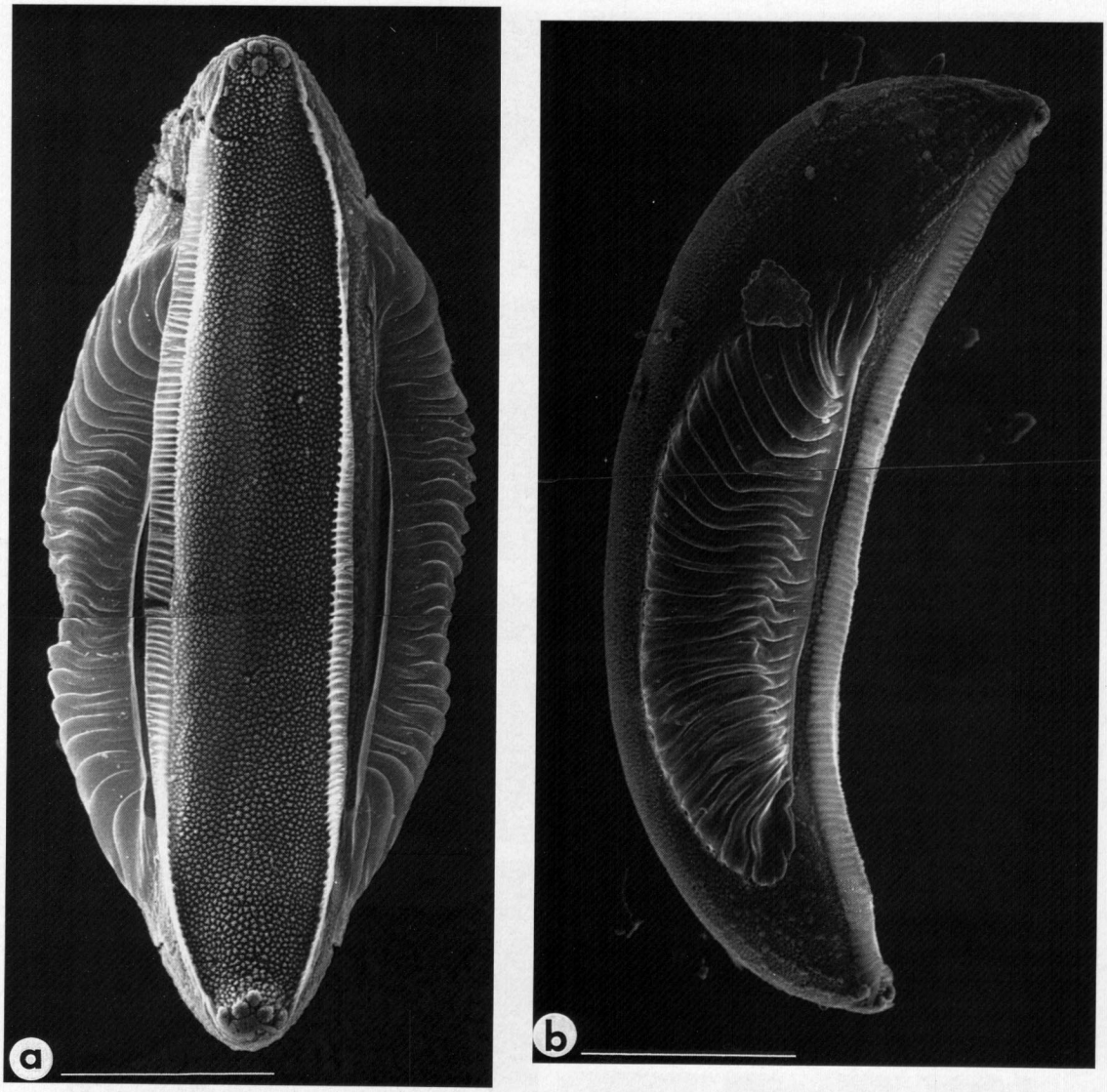

Fig. 7. *Anopheles quadriannulatus* SKUQUA (colony). a. Entire egg, ventral (upper) view, anterior end at top. b. Entire egg, lateral view, ventral surface at right, anterior end at top. Scale = 100 μm.

Principal components and discriminant function analyses

We chose 10 attributes, all but one of which (disk area as a percentage of total micropyle area) had been used previously for multivariate analyses of egg characters because of their independence from egg size or area (Linley et al. 1993a, 1993b, 1995, 1996). Of the 10 principal components derived from the standardized (zero mean, unit variance) variable, the first 4 accounted for 69.0% of the variation and the first 2 for 45.5% of the variation (Table 3). Component 1 carried a heavy positive weighting for area of total deck as a percentage of total egg area, and float length as a percentage of total egg length had the largest negative eigenvector of the first component (Fig. 20). Samples were not separable by species or geography with the first principal component (Fig. 21).

Component 2 accounted for less variance than component 1 (Table 3). Two attributes, mean anterior deck tubercle area and form factor, contributed the most to positive weightings on this axis (Fig. 20). No apparent clustering of points by site (source) was found on this axis (Fig. 21).

Components 3 and 4 accounted for, respectively, 13.1 and 10.4% of total variance. The heaviest weightings on these axes were for anterior tubercle density in component 3 and float length per rib in component 4 (Table 3).

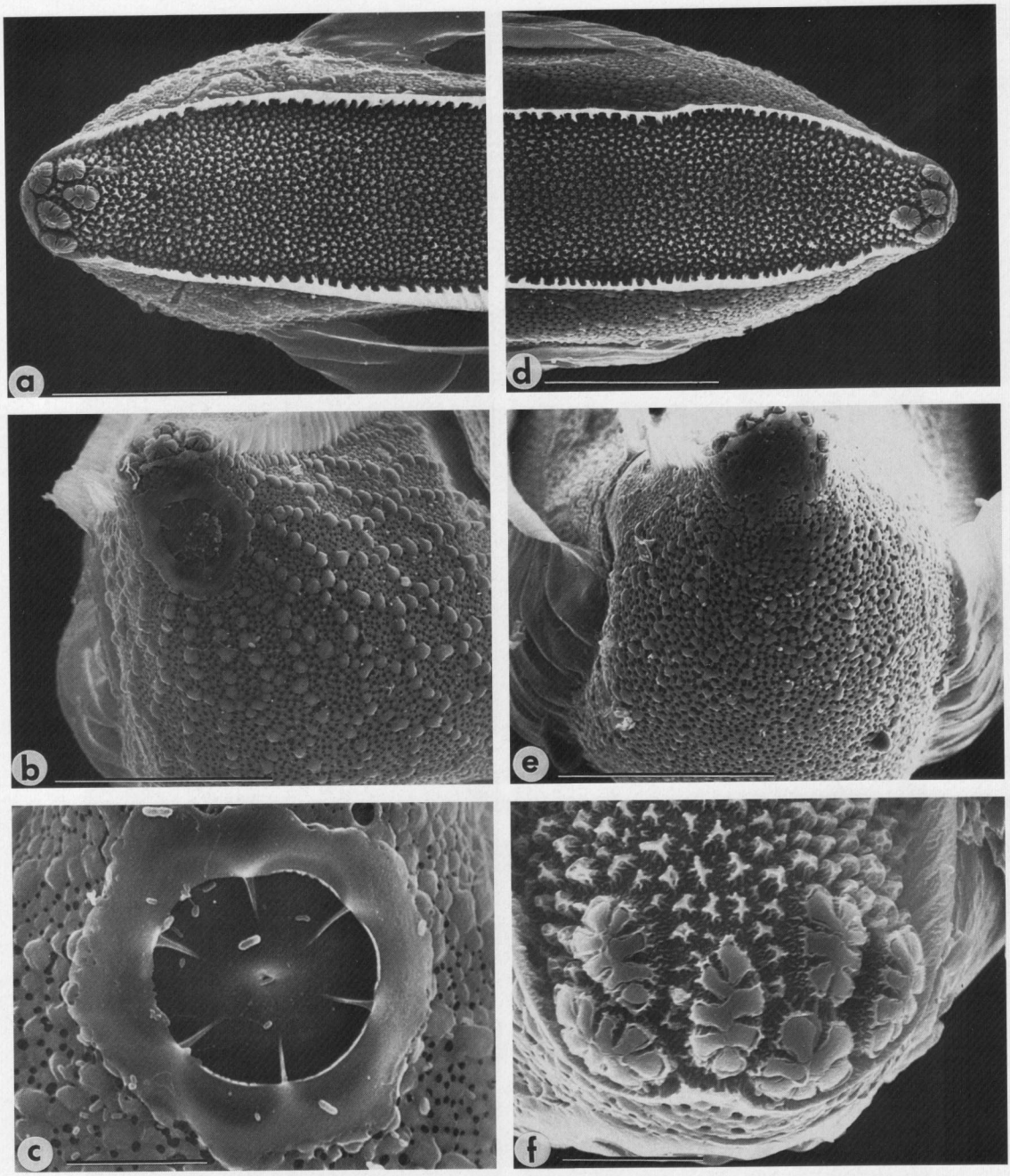

Fig. 8. *Anopheles quadriannulatus* SKUQUA (colony). a. Anterior end, ventral (upper) surface. b. Anterior, end-on view. c. Detail of micropylar apparatus. d. Posterior end, ventral surface. e. Posterior, end-on view. f. Detail, lobed tubercles, anterior end. Scales: a, b, d, e = 50 μm; c, f = 10 μm.

When discriminant analysis was applied to the same 10 variables, 6 significant ($P < 0.001$) functions were derived, of which the first 2 captured 67.2% of the differences among the 12 samples (eggs of the KYA *An. bwambae* were omitted because a float measurement was not done) (Table 4). For discriminant function 1, the saltwater species fell on the negative side and *An. bwambae* and *An. quadriannulatus* were located on the positive side of the axis (Fig. 22). Discriminant function 2 did not clearly separate species. Examining the centroids for each collection source, the MON *An. bwambae* were most distinct from other populations (Fig. 22) and lay closest to *An. quad-*

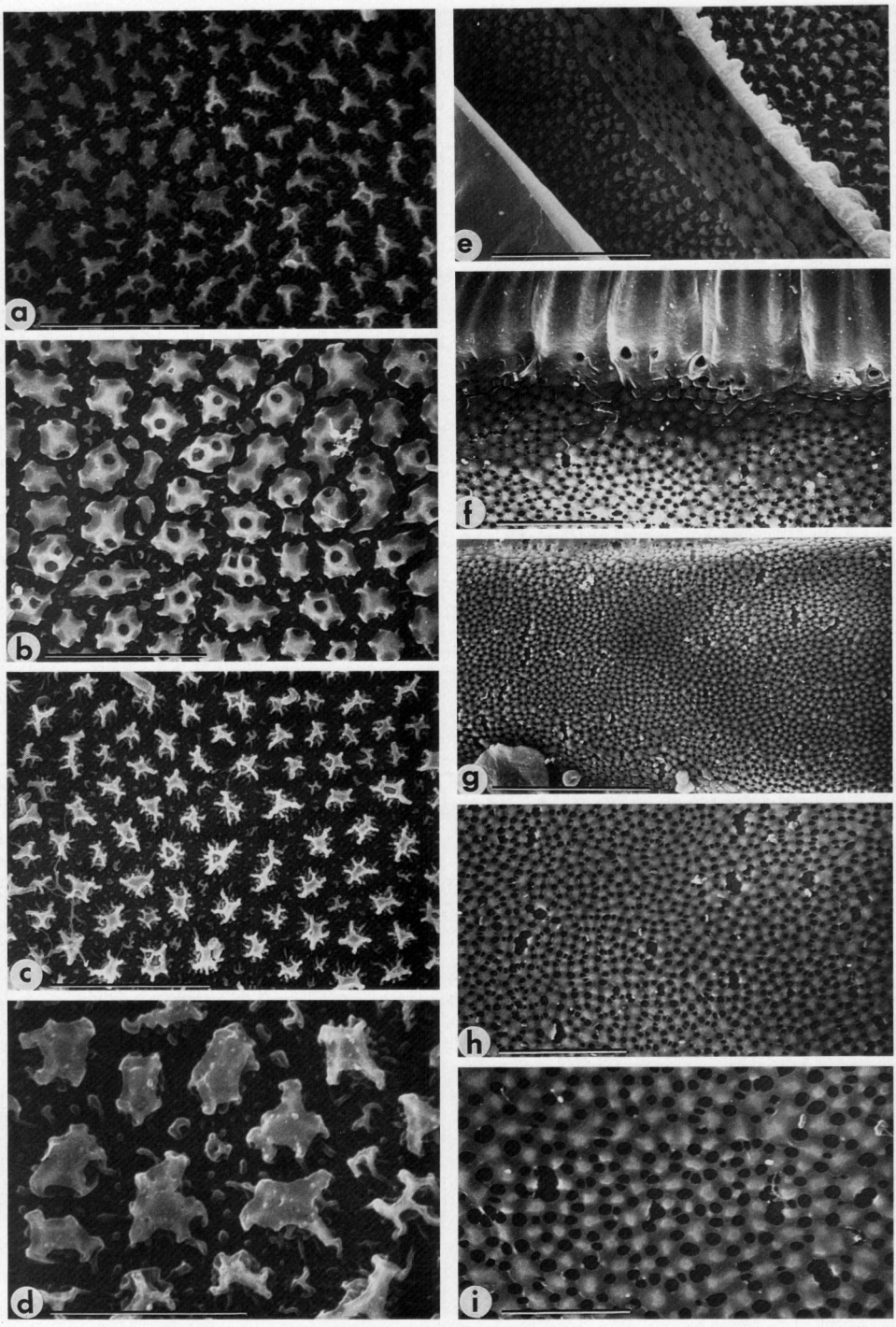

Fig. 9. *Anopheles quadriannulatus* SKUQUA (colony). a. Chorionic tubercles, anterior deck. b. Tubercles, middle deck. c. Tubercles, posterior deck. d. Detail of anterior deck tubercles. e. Plastron between deck and frill (top) and exposed tubercles beneath float (bottom). f. Float dorsal margin and plastron. g. Dorsal surface, middle of egg. h, i. Detail, dorsal surface. Scales: a–c, i = 10 μm; d = 5 μm; e, f, h = 20 μm; g = 50 μm.

Fig. 10. *Anopheles bwambae* MON (progeny of wild-caught females). a. Entire egg, ventral (upper) view, anterior end at top. b. Entire egg, lateral view, ventral surface at right, anterior end at top. Scale = 100 μm.

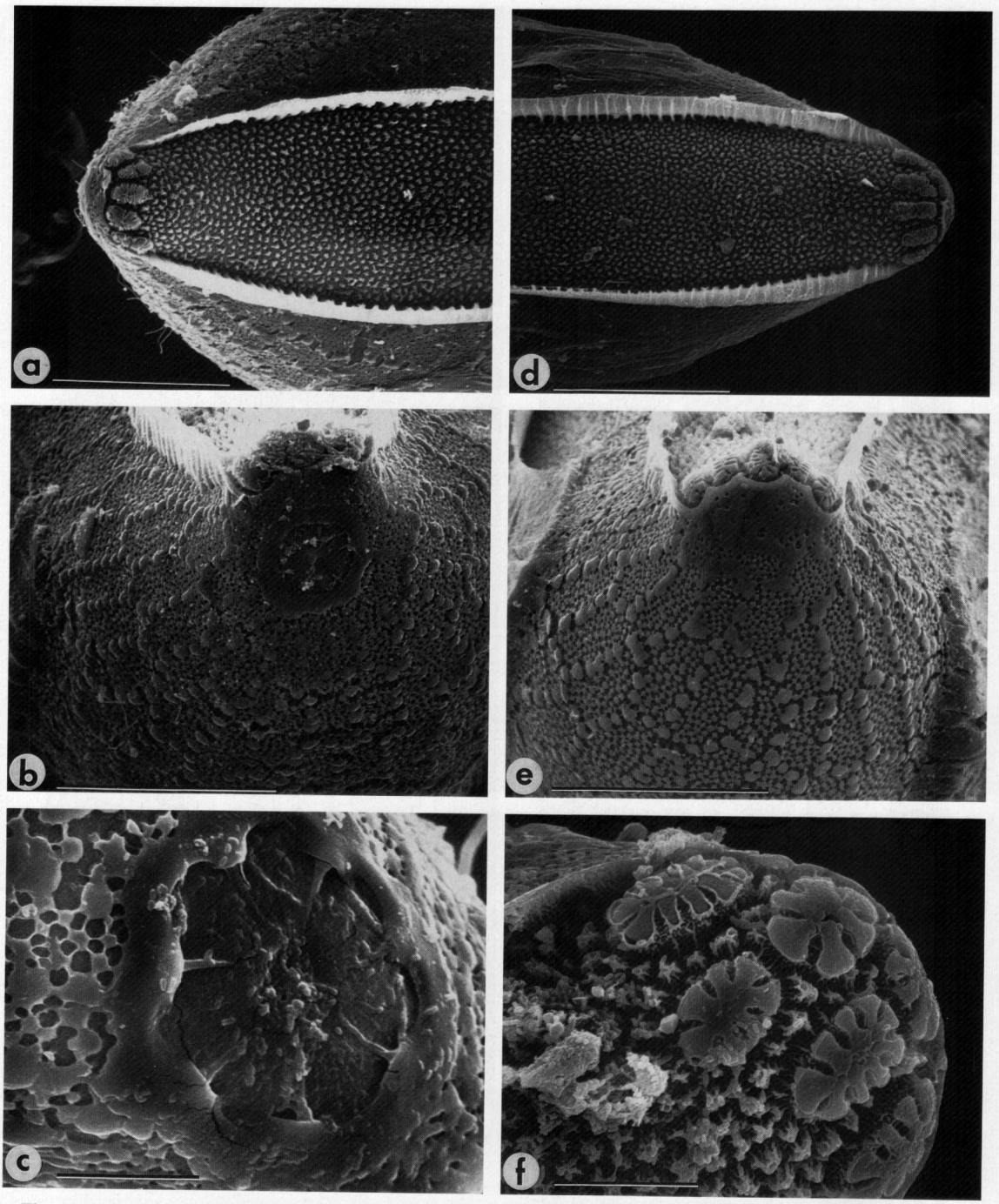

Fig. 11. *Anopheles bwambae* MON (progeny of wild-caught females). a. Anterior end, ventral (upper) surface. b. Anterior, end-on view. c. Detail of micropylar apparatus (small rods are contaminants, probably bacteria). d. Posterior end, ventral surface. e. Posterior, end-on view. f. Detail, lobed tubercles, anterior end. Scales: a, b, d, e = 50 μm; c, f = 10 μm.

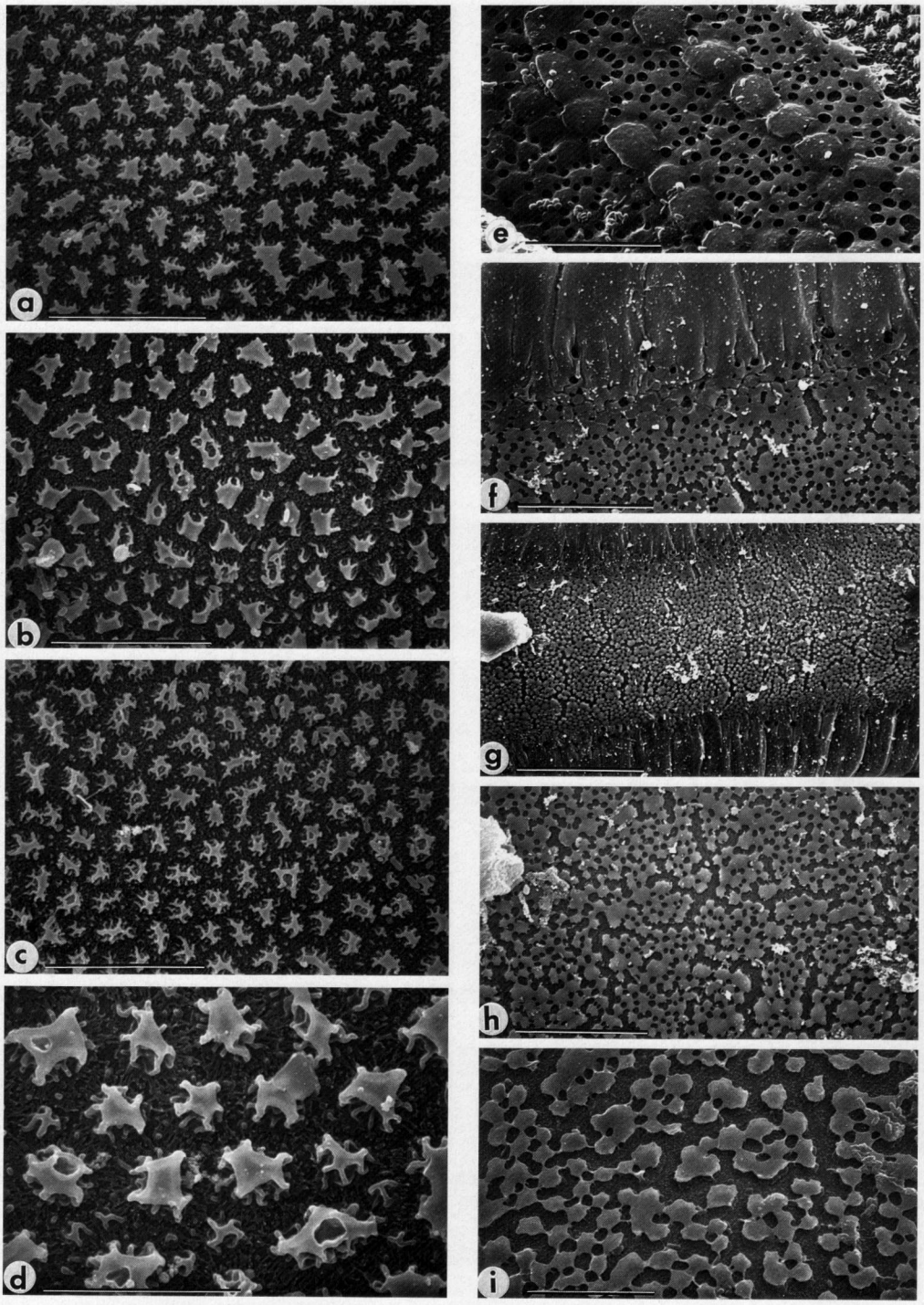

Fig. 12. *Anopheles bwambae* MON (progeny of wild-caught females). a. Chorionic tubercles, anterior deck. b. Tubercles, middle deck. c. Tubercles, posterior deck. d. Detail of anterior deck tubercles. e. Plastron between deck (top) and float (bottom). f. Float dorsal margin. g. Dorsal surface, middle of egg. h, i. Detail, dorsal surface. Scales: a–c, e, i = 10 μm; d = 5 μm; f, h = 20 μm; g = 50 μm.

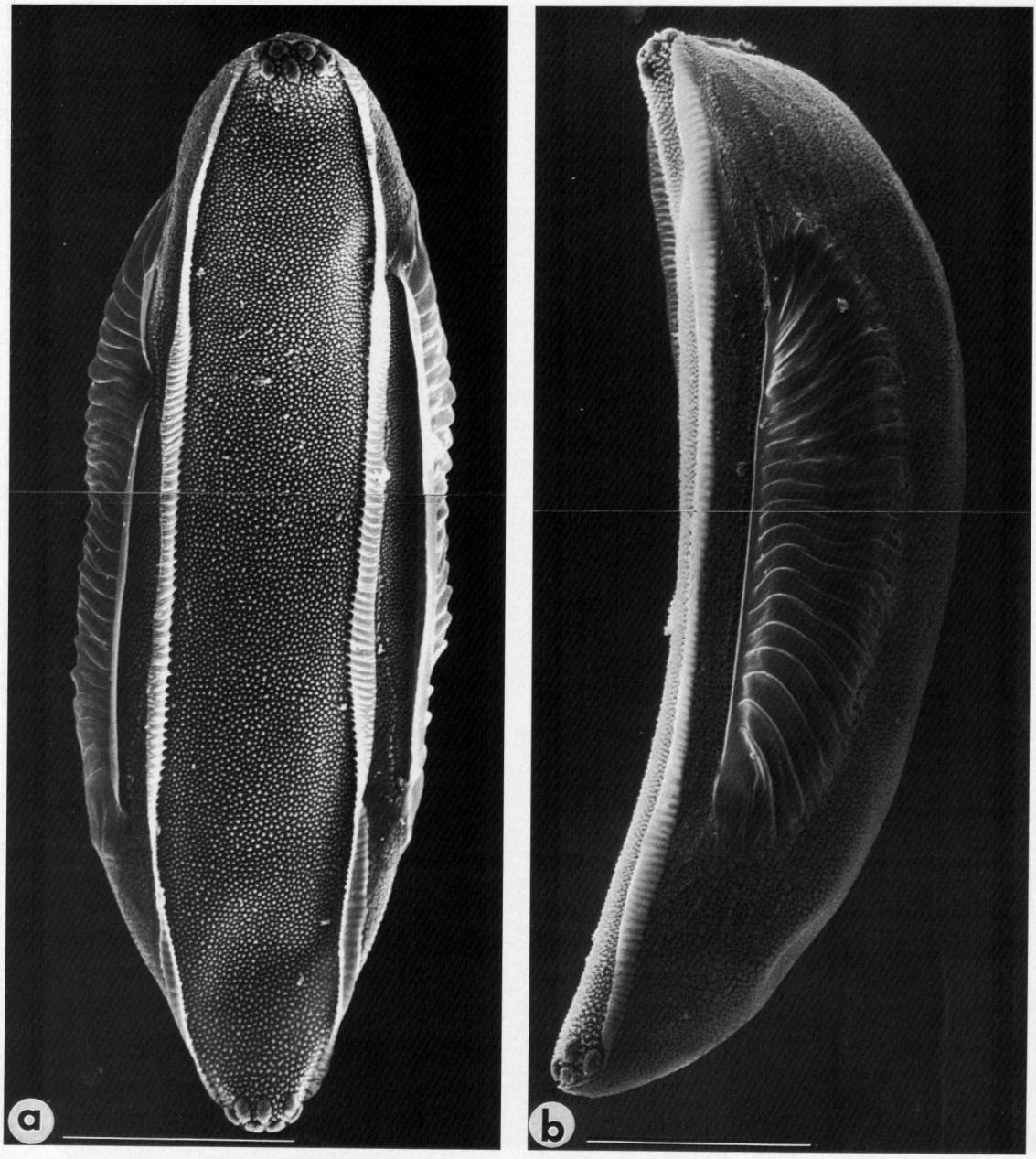

Fig. 13. *Anopheles merus* MERDAR (colony). a. Entire egg, ventral (upper) view, anterior end at top. b. Entire egg, lateral view, dorsal surface at right, anterior end at top. Scale = 100 μm.

riannulatus. The *An. merus* and *An. melas* grouped together on the negative side of function 1, and 3 of the *An. arabiensis* sources (SUD, KGB, KEN) clustered together on the negative side of discriminant function 2. The centroids of the 2 *An. gambiae* (G3, KOG) sources were separated by a greater (Euclidean) distance than any other intraspecific units.

DISCUSSION

Width of the deck region had been used for many years to distinguish eggs of *An. melas* from those of freshwater *An. gambiae* s.l. in West Africa (Muirhead Thomson 1945, 1948, Gelfand 1955), although some freshwater *An. gambiae* from inland Nigeria produced eggs with *melas*-like morphology

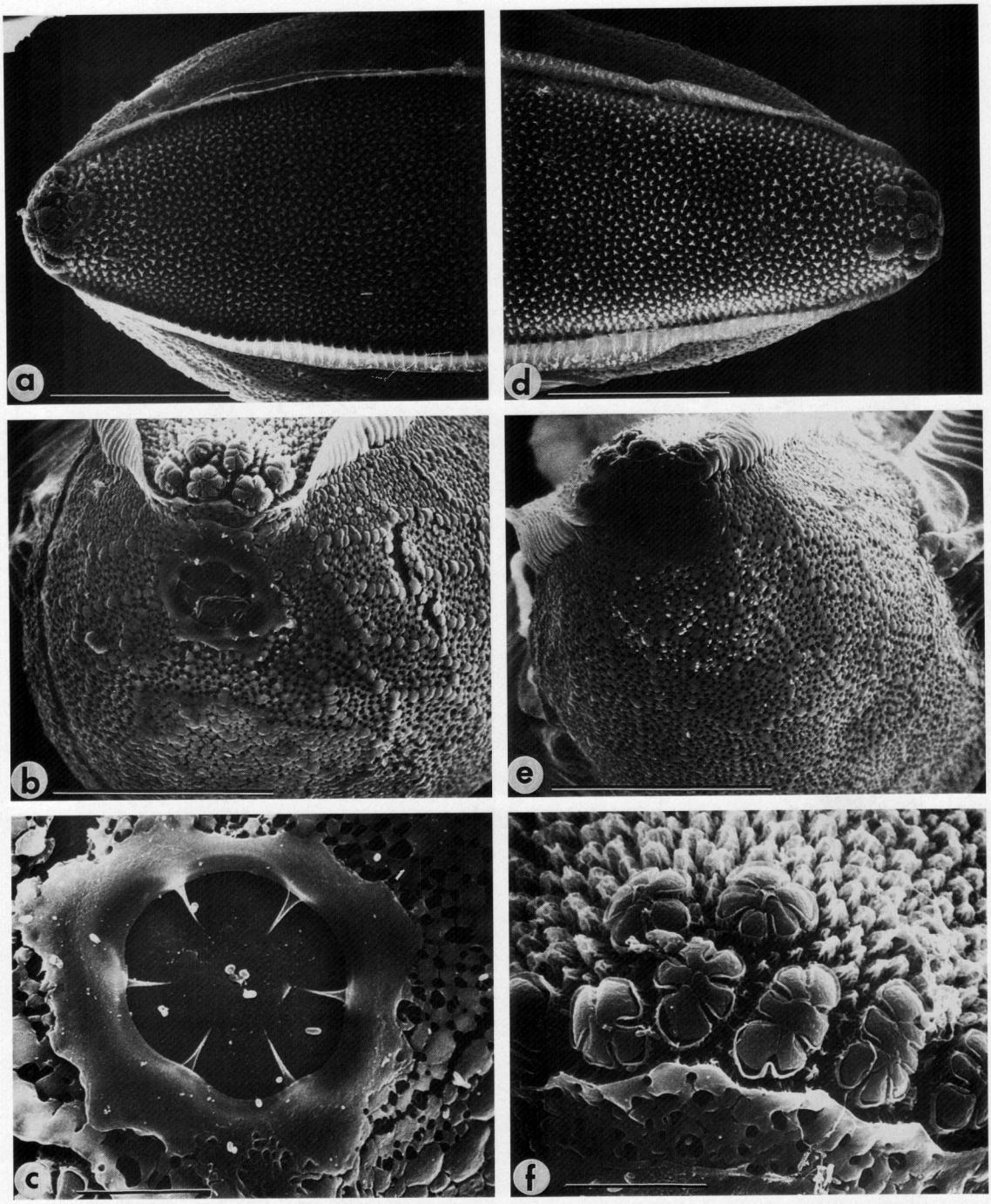

Fig. 14. *Anopheles merus* MERDAR (colony). a. Anterior end, ventral (upper) surface. b. Anterior, end-on view. c. Detail of micropylar apparatus. d. Posterior end, ventral surface. e. Posterior, end-on view. f. Detail, lobed tubercles, anterior end. Scales: a, b, d, e = 50 μm; c, f = 10 μm.

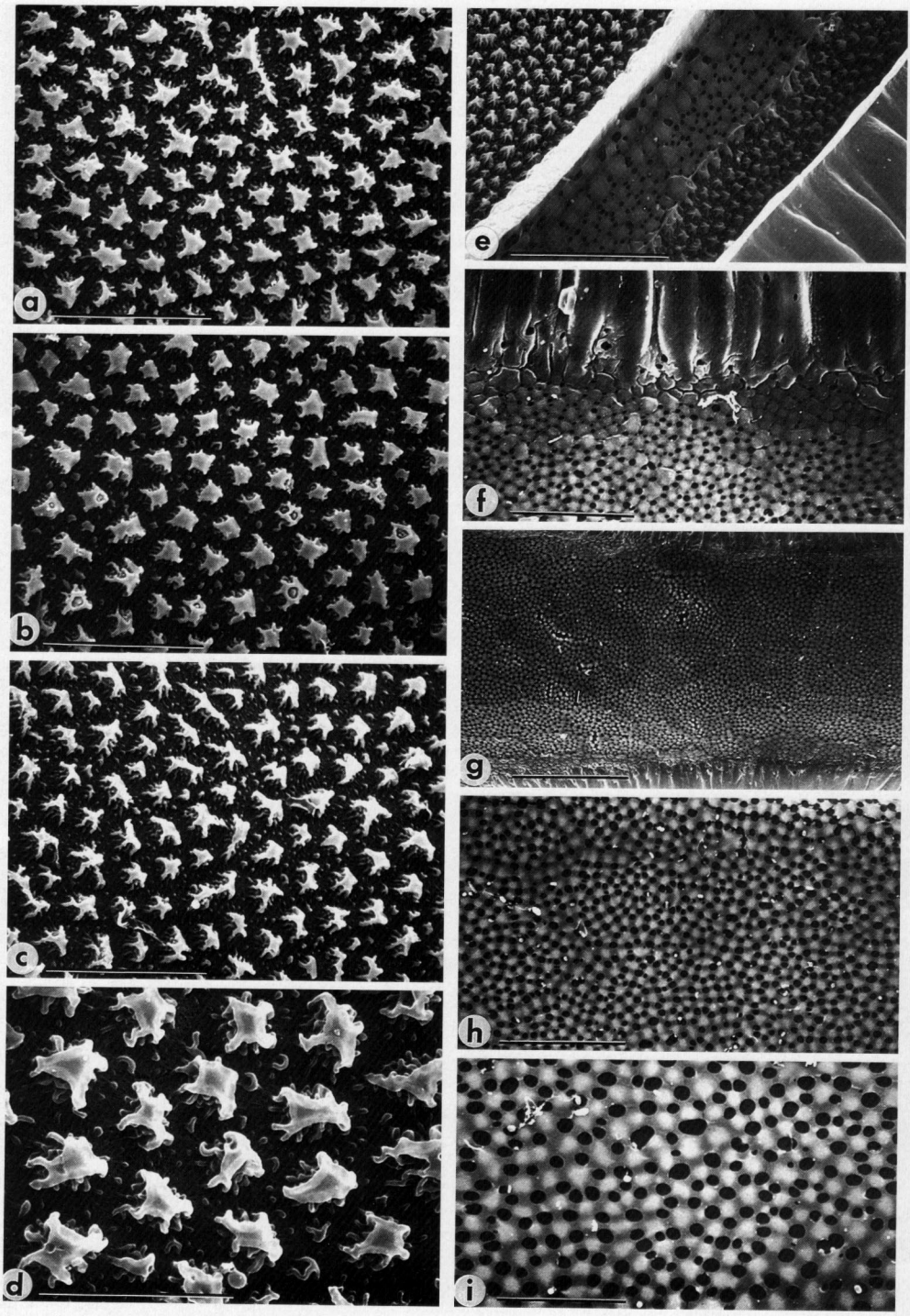

Fig. 15. *Anopheles merus* MERDAR (colony). a. Chorionic tubercles, anterior deck. b. Tubercles, middle deck. c. Tubercles, posterior deck. d. Detail of anterior deck tubercles. e. From left to right: tubercles of upper deck, frill, lateral plastron, tubercles beneath float, float. f. Float dorsal margin to plastron. g. Dorsal surface, middle of egg. h, i. Detail, dorsal surface. Scales: a–c, i = 10 μm; d = 5 μm; e, f, h = 20 μm; g = 50 μm.

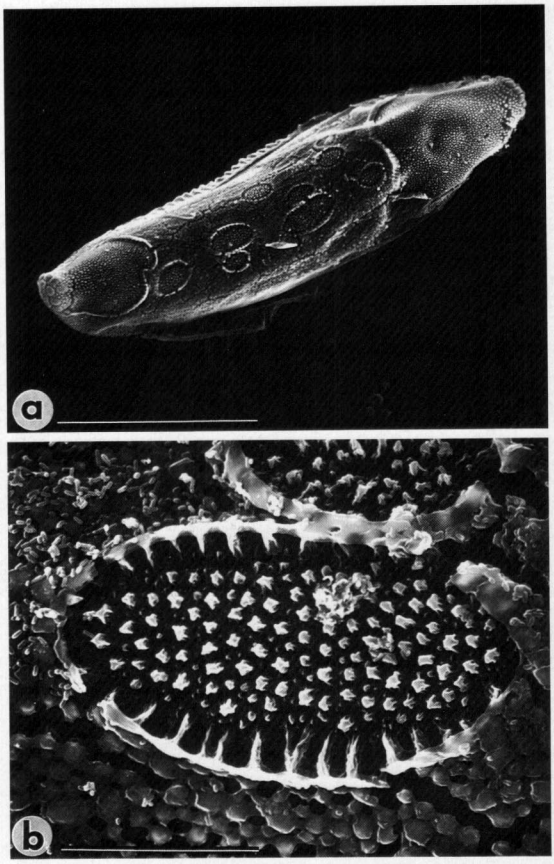

Fig. 16. *Anopheles merus* MERDAR (colony). a. Aberrant form, whole egg. b. Ventral surface of aberrant form, with deck tubercles exposed within ovoid frill. Scales: a = 200 μm; b = 20 μm.

(Bruce-Chwatt and Service 1957). Our measurements indicate that mean deck width as a percentage of total egg width is significantly greater for *An. melas* and *An. merus* than comparable values for most samples of freshwater *An. gambiae* complex used in this study. Light microscope measurements by Coluzzi (1964) indicated that mean egg length and width of *An. melas* and *An. merus* were significantly greater than those of *An. gambiae* 'A' (=*An. gambiae* s.s.) or 'B' (=*An. arabiensis*), but significant differences in our results applied to only 2 sources of *An. arabiensis* (SUD, DAKAR) and one of *An. gambiae* (KOG).

Curiously, Hinton (1968), in the only previous SEM study that included eggs of the *An. gambiae* complex, noted that saltwater forms of anopheline species generally have smaller eggs with proportionally smaller floats and fewer ribs than freshwater forms. Our results confirm the latter 2 generalizations, in that means of float length as a percentage of total egg length and mean number of ribs were significantly less for *An. merus* and *An. melas* than for most sources of *An. arabiensis, An. gambiae,* and *An. quadriannulatus.* Other quantifications of Hinton (1968) indicated a difference in the number of anterior versus posterior lobed tubercles for *An. gambiae* (6 vs. 5), but not for *An. merus* (5 vs. 5). Our results show a general trend of more anterior than posterior lobed tubercles among all 6 species of *An. gambiae* (Table 2). However, we cannot confirm, as claimed by Hinton (1968), that *An. gambiae* eggs have more micropylar ridges (7) than *An. melas* (6), because the number of sectors showed no significant differences among species.

Our discovery of aberrant eggs among colony *An. merus* is preceded by a much earlier report of abnormal eggs from colonized *An. gambiae* s.l. (Deane and Causey 1943). These authors designated 1.4% of 12,525 eggs examined as abnormal, including a form whose deck region was patchily covered by plastron, as in our *An. merus* (Fig. 16). Aberrant egg forms were recovered more often from colonized *Anopheles albimanus* Wiedemann than from wild-caught females (Rodriguez et al. 1992). The observations of abnormal eggs in colonies of 3 *Anopheles* species may not be representative of naturally occurring polymorphisms of anopheline eggs in nature.

Eggs of a relatively large number of species of *Anopheles* have now been examined by SEM, opening the way for morphologic comparisons among taxa, such as subgenera. For example, lobed tubercles occur at posterior and anterior ends of all species of *Cellia* examined to date (Hinton 1968, this study), *Kerteszia* (Forattini et al. 1997), and most species of subgenus *Anopheles* (e.g., Linley et al. 1993a, 1995 but note exceptions in Linley and Lounibos 1994, Lounibos et al. 1997b). However, lobed tubercles are absent from all *Anopheles* (*Nyssorhynchus*) eggs (e.g., Linley et al. 1993b, 1996; Forattini et al. 1997; Lounibos et al. 1997a).

The present work is the 5th in a series that applies multivariate statistical methods to egg attributes of anopheline species groups (Linley et al. 1995), complexes (Linley et al 1993a), or geographic populations within species (Linley et al. 1993b, 1996). Attributes that were most important in the 1st and 2nd principal components, such as area of total deck as a percentage of whole egg area and mean float length as a percentage of egg length, were the same in the present and in most past studies. However, the discriminatory powers of previous studies were greater for distinguishing closely related species, such as the species of the *An. quadrimaculatus* complex (Linley et al. 1993a) or of the Hyrcanus Group of *Anopheles* (Linley et al. 1995). The poorer resolving powers of egg structures for species of the *An. gambiae* complex may be attributable to the closer genetic relationships of these species and more geographic and colony variation in the current study compared to previously published works.

Fig. 17. *Anopheles melas* DJ1 (progeny of wild-caught females). a. Entire egg, ventral (upper) view, anterior end at top. b. Entire egg, lateral view, ventral surface at left, anterior end at top. Scale = 100 μm.

Recent comparisons of DNA sequences of the *An. gambiae* complex have led to a revision of presumed phylogenetic relationships among species, previously based on chromosomal arrangements (Besansky et al. 1994). Our results, based on discriminant function analyses of egg attributes, are consistent with the interpretations from molecular data of close relationships between *An. gambiae* s.s. and *An. arabiensis* and between *An. merus* and *An. melas* (Fig. 22). Although *An. bwambae* was not

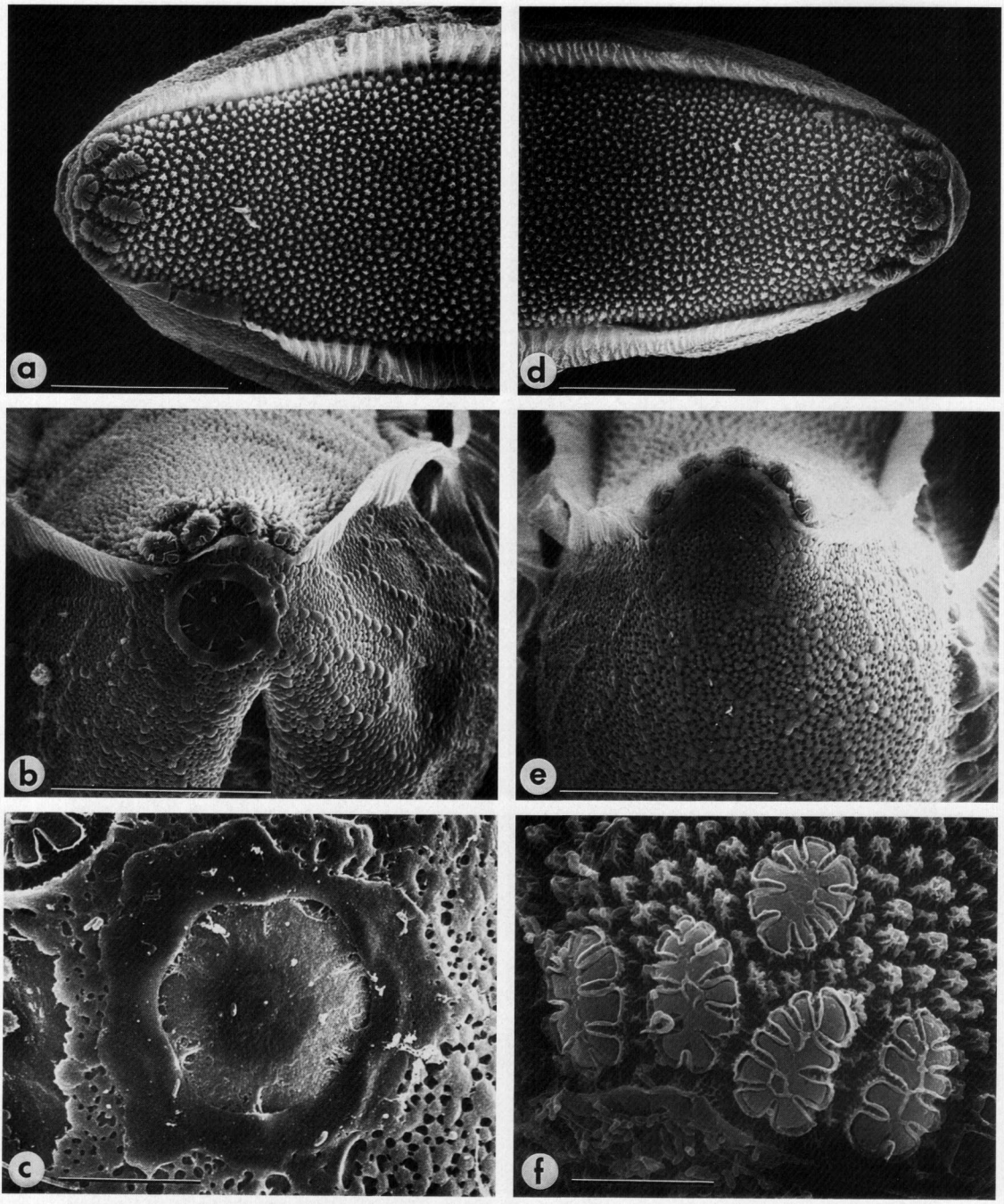

Fig. 18. *Anopheles melas* DJI (progeny of wild-caught females). a. Anterior end, ventral (upper) surface. b. Anterior, end-on view (open wedge is a break in the chorion.). c. Detail of micropylar apparatus (orifice is occluded by unknown substance.). d. Posterior end, ventral surface. e. Posterior, end-on view. f. Detail, lobed tubercles, anterior end. Scales: a, b, d, e = 50 μm; c, f = 10 μm.

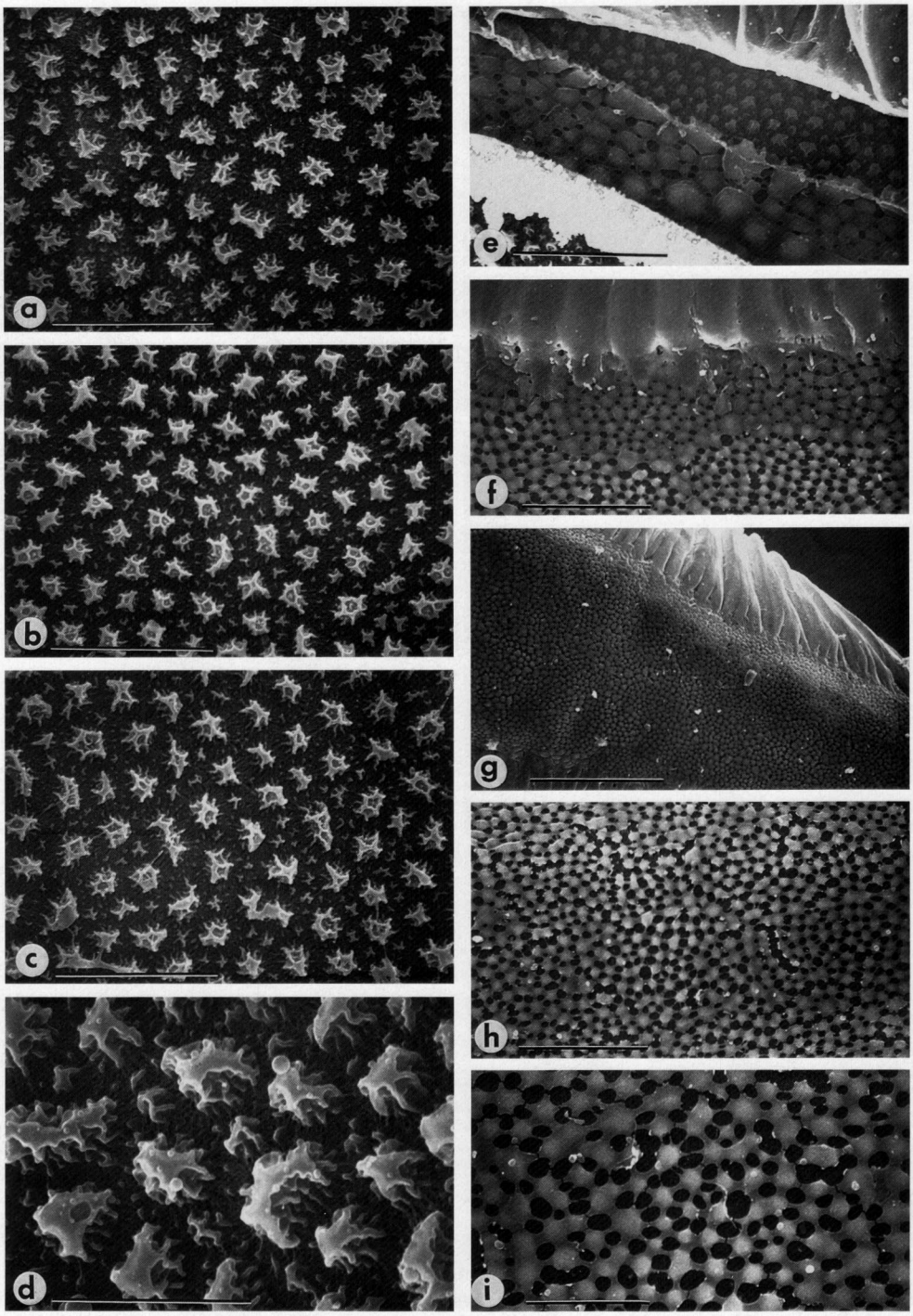

Fig. 19. *Anopheles melas* DJI (progeny of wild-caught females). a. Chorionic tubercles, anterior deck. b. Tubercles, middle deck. c. Tubercles, posterior deck. d. Detail of anterior deck tubercles. e. From bottom to top: tubercles of upper deck, frill, plastron, tubercles beneath float, float. f. Float dorsal margin to dorsal plastron. g. Dorsal surface, middle of egg. h, i. Detail, dorsal surface. Scales: a–c, i = 10 μm; d = 5 μm; e, f, h = 20 μm; g = 50 μm.

Table 3. Partial tabulation of principal components analysis of 10 attributes of *Anopheles gambiae* complex eggs from 13 sources.

Principal component	Eigenvalue	% variance explained	Attribute[1]									
			Lenwidrt	Fltpcn	Fltenprib	Totdkpcn	Totnolobtb	Dkwidpcdn	Mnanttbar	Mnanttbfm	Anttbden	Dskarpcn
1	2.70	27.0	0.291	−0.413	−0.026	0.473	0.348	0.356	−0.317	−0.261	0.316	0.053
2	1.85	18.5	0.250	−0.092	0.328	0.308	0.039	0.337	0.532	0.449	−0.326	0.143
3	1.31	13.1	−0.177	0.421	0.290	−0.122	0.423	0.070	−0.129	0.362	0.486	0.353
4	1.04	10.4	0.245	0.258	0.575	0.020	−0.035	0.013	−0.205	−0.032	0.037	−0.704

[1] Attributes are defined in the Appendix.

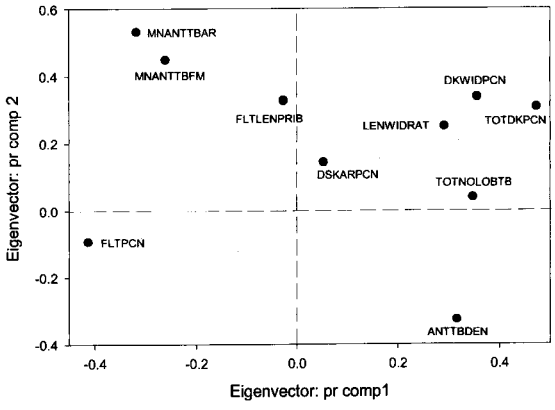

Fig. 20. Plot of the eigenvectors of the 1st 2 principal components based on 10 attributes of eggs measured from 13 sources of 6 species of the *Anopheles gambiae* complex. Abbreviations of attributes are explained in the Appendix.

included in the analyses of Besansky et al. (1994), it may be noteworthy that this species produces fertile male offspring in the interspecific cross with *An. quadriannulatus* (Davidson and White 1972), with which species it shares the greatest chromosomal homology (Davidson and Hunt 1973). A close genetic relationship between these species is consistent with similarities revealed by discriminant function analysis of egg attributes (Fig. 22).

The greatest intraspecific divergence in egg morphology was observed between colony samples of *An. gambiae* s.s that originated from West (G3) and East (KOG) Africa. Because *An. gambiae* s.s. in West Africa is known to comprise several different species (Coluzzi 1984, Favia et al. 1997), some of the egg morphologic characters may be due to interspecific differences or they may simply be attributable to inadvertent selection in laboratory colonies, one of which is several decades old (Table 1). Artificial selection in colonies, geographic variation, and cryptic species within *An. arabiensis* (Coetzee 1997) may also be involved in the variability observed among eggs of this species from 5 sources.

Table 4. Summary of significant ($P < 0.001$) discriminant functions from analyses of 10 attributes of eggs from 12 sources of *Anopheles gambiae* complex mosquitoes.

Function no.	Eigenvalue	Percentage	χ^2	df	P
1	4.459	47.6	573.8	110	<0.0001
2	1.840	19.6	382.0	90	<0.0001
3	1.223	12.0	264.1	72	<0.0001
4	0.763	8.1	179.0	56	<0.0001
5	0.548	5.9	114.9	42	<0.0001
6	0.297	3.2	65.5	30	<0.001

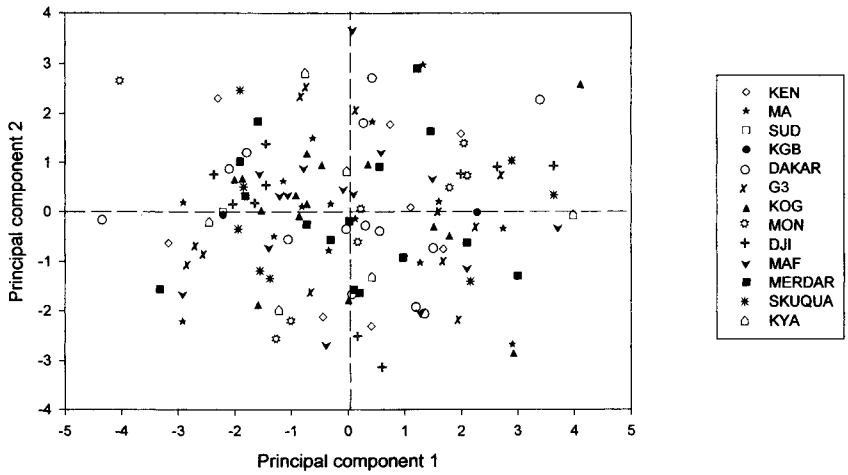

Fig. 21. Plot of the 1st 2 components for each individual egg. Species and source codes are given in Table 1.

ACKNOWLEDGMENTS

We thank A. Diop for collections from Senegal. This work was supported in part by a grant from the National Institutes of Health (AI-31034) and is Florida Agricultural Experiment Station Journal Series R-06784.

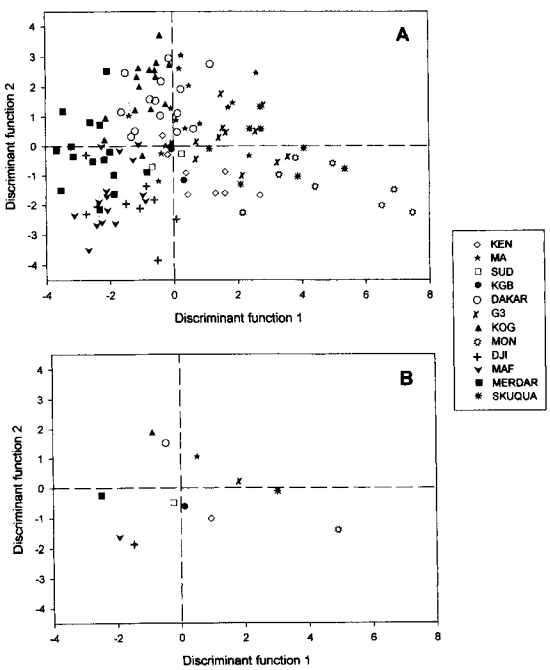

Fig. 22. A. Plot of the first 2 individual discriminant functions, based on 10 attributes, of 123 eggs from 12 sources of the 6 named species of the *Anopheles gambiae* complex. B. Group centroids, by egg source, for the data plotted in A. Source codes are given in Table 1.

REFERENCES CITED

Besansky, N. J., J. R. Powell, A. Caccone, D. M. Hamm, J. A. Scott and F. H. Collins. 1994. Molecular phylogeny of the *Anopheles gambiae* complex suggests genetic introgression between principal malaria vectors. Proc. Natl. Acad. Sci. USA 91:6885–6888.

Bruce-Chwatt, L. J. and M. W. Service. 1957. An aberrant form of *Anopheles gambiae* Giles from southern Nigeria. Nature 179:873.

Coetzee, M. 1989. Comparative morphology and multivariate analysis for the discrimination of four members of the *Anopheles gambiae* group in southern Africa. Mosq. Syst. 21:100–116.

Coetzee, M. 1997. Morphological and genetic variation within populations of *Anopheles arabiensis* Patton from southern Africa (Diptera: Culicidae). Mem. Entomol. Soc. Wash. 18:95–100.

Coluzzi, M. 1964. Morphological divergences in the *Anopheles gambiae* complex. Riv. Malariol. 43:197–232.

Coluzzi, M. 1984. Heterogeneities of the malaria vectorial system in tropical Africa and their significance in malaria epidemiology and control. Bull. WHO 62:107–113.

Coluzzi, M. and A. Sabatini. 1967. Cytogenetic observations on species A and B of the *Anopheles gambiae* complex. Parassitologia 9:73–88.

Coluzzi, M., V. Petrarca and M. A. Di Deco. 1985. Chromosomal inversion, intergradation and incipient speciation in *Anopheles gambiae*. Boll. Zool. 52:45–63.

Davidson, G. and R. H. Hunt. 1973. The crossing and chromosome characteristics of a new, sixth species in the *Anopheles gambiae* complex. Parassitologia 15: 121–128.

Davidson, G. and G. B. White. 1972. The crossing characteristics of a new, sixth species in the *Anopheles gambiae* complex. Trans. R. Soc. Trop. Med. Hyg. 66:531–532.

Deane, M. P. and O. R. Causey. 1943. Viability of *Anopheles gambiae* eggs and morphology of unusual types found in Brazil. Am. J. Trop. Med. 23:95–103.

Favia, G., A. della Torre, M. Bagayoko, A. Lanfrancotti,

N. F. Sagnon, Y. T. Toure and M. Coluzzi. 1997. Molecular identification of sympatric chromosomal forms of *Anopheles gambiae* and further evidence of their reproductive isolation. Insect Mol. Biol. 6:377–383.

Forattini, O. P., M. A. M. Sallum, G. R. A. M. Marques and D. C. Flores. 1997. Description of the eggs of *Anopheles* (*Kerteszia*) *laneanus* and *Anopheles* (*Nyssorhynchus*) *antunesi* (Diptera: Culicidae) by scanning electron microscopy. J. Am. Mosq. Control Assoc. 13: 368–374.

Gelfand, H. M. 1955. *Anopheles gambiae* Giles and *Anopheles melas* Theobald in a coastal area of Liberia, West Africa. Trans. R. Soc. Trop. Med. Hyg. 49:508–527.

Gillies, M. T. and M. Coetzee. 1987. A supplement to the Anophelinae of Africa south of the Sahara. Publ. S. Afr. Inst. Med. Res. Publication number 55.

Hinton, H. E. 1968. Observations on the biology and taxonomy of the eggs of *Anopheles* mosquitoes. Bull. Entomol. Res. 57:495–508.

Hunt, R. H. 1973. A cytological technique for the study of the *Anopheles gambiae* complex. Parassitologia 15: 137–139.

Hunt, R. H., M. Coetzee and M. Fettene. 1998. The *Anopheles gambiae* complex: a new species from Ethiopia. Trans. R. Soc. Trop. Med. Hyg. 92:231–235.

Linley, J. R. and L. P. Lounibos. 1994. The remarkable egg of *Anopheles peryassui* (Diptera: Culicidae). Mosq. Syst. 26:25–34.

Linley, J. R., P. E. Kaiser and A. F. Cockburn. 1993a. A description and morphometric study of the eggs of species of the *Anopheles quadrimaculatus* complex (Diptera: Culicidae). Mosq. Syst. 25:124–147.

Linley, J. R., L. P. Lounibos and J. Conn. 1993b. A description and morphometric analysis of the eggs of four South American populations of *Anopheles* (*Nyssorhynchus*) *aquasalis* (Diptera: Culicidae). Mosq. Syst. 25: 198–214.

Linley, J. R., H. H. Yap and T. B. Damar. 1995. The eggs of four species of the *Anopheles hyrcanus* Group in Malaysia. Mosq. Syst. 27:43–71.

Linley, J. R., L. P. Lounibos, J. Conn, D. Duzak and N. Nishimura. 1996. A description and morphometric comparison of eggs from eight geographic populations of the South American malaria vector *Anopheles* (*Nyssoryhnchus*) *nuneztovari* (Diptera: Culicidae). J. Am. Mosq. Control Assoc. 12:275–292.

Lounibos, L. P., D. Duzak and J. R. Linley. 1997a. Comparative egg morphology of six species of the Albimanus Section of *Anopheles* (*Nyssorhynchus*) (Diptera: Culicidae). J. Med. Entomol. 34:136–155.

Lounibos, L. P., D. Duzak, J. R. Linley and R. Lourenço-de-Oliveira. 1997b. Egg structures of *Anopheles fluminensis* and *Anopheles shannoni*. Mem. Inst. Oswaldo Cruz Rio de J. 92:221–232.

Muirhead Thomson, R. C. 1945. Studies on the breeding places and control of *Anopheles gambiae* and *A. gambiae* var. *melas* in coastal districts of Sierra Leone. Bull. Entomol. Res. 36:185–252.

Muirhead Thomson, R. C. 1948. Studies on *Anopheles gambiae* and *A. melas* in and around Lagos. Bull. Entomol. Res. 38:527–558.

Rodriguez, M. H., B. Chavez, A. Orozco, E. G. Loyola and A. Martinez-Palomo. 1992. Scanning electron microscopic observations of *Anopheles albimanus* (Diptera: Culicidae) eggs. J. Med. Entomol. 29:400–406.

SAS Institute Inc. 1985. SAS user's guide: statistics. Version 5 edition. SAS Institute Inc., Cary, NC.

Scott, J. A., W. G. Brogdon and F. H. Collins. 1993. Identification of single specimens of the *Anopheles gambiae* complex by the polymerase chain reaction. Am. J. Trop. Med. Hyg. 49:520–529.

Statgraphics. 1992. Reference manual. Version 6 edition. Manguistics Inc., Rockville, MD.

White, G. B. 1974. *Anopheles gambiae* complex and disease transmission in Africa. Trans. R. Soc. Trop. Med. Hyg. 68:278–301.

APPENDIX

Definitions of abbreviations of measured or calculated attributes of eggs of the *Anopheles gambiae* complex.

Abbreviation	Attribute
Antposlobrat	Ratio of number anterior/posterior lobed tubercles
Anttbden	Anterior deck tubercule density
Artotdk	Area of total deck
Arwhlegg	Area of whole egg (ventral view)
Colarmic	Collar area of micropyle
Dkwipdcn	Width of deck as % egg width
Dskarmic	Disk area of micropyle
Dskarpcn	Disk area as % total micropylar apparatus area
Egglen	Egg length
Eggwid	Egg width (widest point, across floats)
Fltlenprib	Float length/total number of ribs
Fltpcn	Float length as % of egg length
Lenwidrat	Length/width ratio
Mnanttbar	Mean anterior deck tubercle area
Mnanttbfm	Mean anterior deck tubercle form factor
Mnfltlen	Mean float length (of the 2 floats)
Mnribs	Mean number of ribs (of the 2 floats)
Noantlobtb	Number of anterior lobed tubercles
Noposlobtb	Number of posterior lobed tubercles
Nosect	Number of sectors in micropylar disk
Totarmic	Total area of micropylar apparatus
Totdkpcn	Area of total deck as % area whole egg
Totnolobtb	Total number of lobed tubercles